AD-A144 525 INVESTIGATION OF ION BEAM PRODUCTION AND ACCELERATION 1/1
USING LINEAR ELECTR..(U) MARYLAND UNIV COLLEGE PARK
DEPT OF ELECTRICAL ENGINEERING MAR 84 AFOSR-TR-84-0641
UNCLASSIFIED AFOSR-83-0145 F/G 20/7 NL

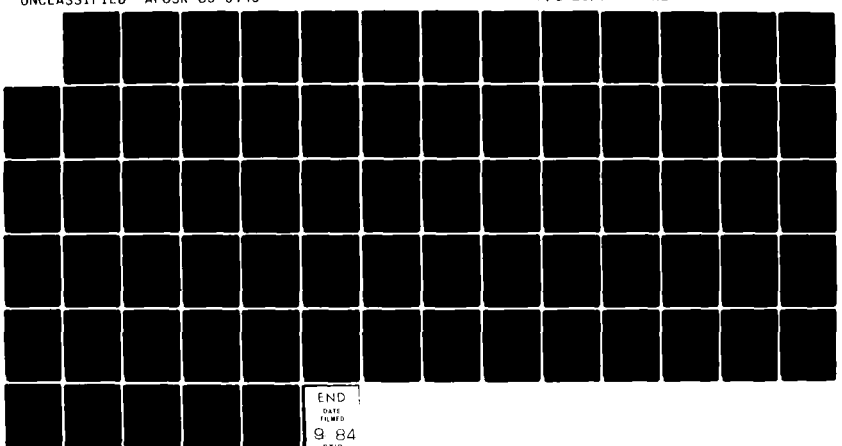

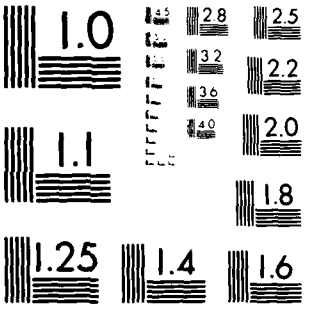

INVESTIGATION OF ION BEAM PRODUCTION AND ACCELERATION USING LINEAR ELECTRON BEAMS AND A PULSE POWERED PLASMA FOCUS

Contract No. AFOSR-83-0145

Final PROGRESS REPORT

For the Period April 1, 1983 through March 31, 1984

Submitted to

Air Force Office of Scientific Research

Prepared by

Charged Particle Beam Research Group
Electrical Engineering Department
University of Maryland
College Park, Maryland 20742

UNCLASSIFIED

SECURITY CLASSIFICATION OF THIS PAGE

REPORT DOCUMENTATION PAGE

1a. REPORT SECURITY CLASSIFICATION: UNCLASSIFIED	1b. RESTRICTIVE MARKINGS
2a. SECURITY CLASSIFICATION AUTHORITY	3. DISTRIBUTION/AVAILABILITY OF REPORT: Approved for public release; distribution unlimited.
2b. DECLASSIFICATION/DOWNGRADING SCHEDULE	
4. PERFORMING ORGANIZATION REPORT NUMBER(S)	5. MONITORING ORGANIZATION REPORT NUMBER(S): AFOSR-TR- [illegible]
6a. NAME OF PERFORMING ORGANIZATION: Univ. Maryland/Drestler; 6b. OFFICE SYMBOL (If applicable)	7a. NAME OF MONITORING ORGANIZATION: AIR FORCE OFFICE OF SCIENTIFIC RESEARCH
6c. ADDRESS (City, State and ZIP Code): Electrical Engineering Dept. College Park, MD 20742	7b. ADDRESS (City, State and ZIP Code): Bolling AFB, DC 20332
8a. NAME OF FUNDING/SPONSORING ORGANIZATION: AFOSR; 8b. OFFICE SYMBOL (If applicable): NP	9. PROCUREMENT INSTRUMENT IDENTIFICATION NUMBER: AFOSR-83-0145
8c. ADDRESS (City, State and ZIP Code): Bolling AFB, DC 20332	10. SOURCE OF FUNDING NOS.

PROGRAM ELEMENT NO.	PROJECT NO.	TASK NO.	WORK UNIT NO.
61102F	2301	A7	

11. TITLE (Include Security Classification): Investigation of Ion Beam Production and Acceleration Using Linear Electron Beams and a Pulse Powered Plasma Focus

12. PERSONAL AUTHOR(S): Drestler

13a. TYPE OF REPORT	13b. TIME COVERED	14. DATE OF REPORT (Yr., Mo., Day)	15. PAGE COUNT
final	FROM 1Apr83 TO 31Mar84	Mar 84	70

16. SUPPLEMENTARY NOTATION

17. COSATI CODES			18. SUBJECT TERMS (Continue on reverse if necessary and identify by block number)
FIELD	GROUP	SUB. GR.	

19. ABSTRACT (Continue on reverse if necessary and identify by block number)

An intense relativistic electron beam cannot propagate in a metal drift tube when the current exceeds the space charge limit. Very high charge density and electric field gradients (10^2 to 10^3 MV/m) develop at the beam front and the electrons are reflected. When a neutral gas or a plasma is present, collective acceleration of positive ions occur, and the resulting charge neutralization enables the beam to propagate. Experimental results, theoretical understanding, and schemes to achieve high ion energies by external control of the beam front velocity will be reviewed.

20. DISTRIBUTION/AVAILABILITY OF ABSTRACT	21. ABSTRACT SECURITY CLASSIFICATION
UNCLASSIFIED/UNLIMITED ☒ SAME AS RPT. ☐ DTIC USERS ☐	UNCLASSIFIED

22a. NAME OF RESPONSIBLE INDIVIDUAL	22b. TELEPHONE NUMBER (Include Area Code)	22c. OFFICE SYMBOL
Maj. Henry Pugh	(202) 767-4907	NP

DD FORM 1473, 83 APR EDITION OF 1 JAN 73 IS OBSOLETE.

UNCLASSIFIED

SECURITY CLASSIFICATION OF THIS PAGE

INVESTIGATION OF ION BEAM PRODUCTION AND ACCELERATION USING LINEAR ELECTRON BEAMS AND A PULSE POWERED PLASMA FOCUS

Contract No. AFOSR-83-0145

PROGRESS REPORT

For the Period April 1, 1983 through March 31, 1984

Submitted to

Air Force Office of Scientific Research

Prepared by [illegible]
Chief, [illegible]

Charged Particle Beam Research Group
Electrical Engineering Department
University of Maryland
College Park, Maryland 20742

PROGRESS REPORT

SUBMITTED TO:	Air Force Office of Scientific Research
SUBMITTED BY:	Electrical Engineering Department University of Maryland College Park, Maryland 20742
GRANT NUMBER:	AFOSR-83-0145
AMOUNT:	$119,587.00
PERIOD:	April 1, 1983 through March 31, 1984
PRINCIPAL INVESTIGATORS:	William W. Destler, Associate Professor Electrical Engineering Department Martin P. Reiser, Professor Electrical Engineering Department and Department of Physics and Astronomy Moon-Jhong Rhee, Professor Electrical Engineering Department Charles D. Striffler, Associate Professor Electrical Engineering Department
TITLE OF RESEARCH PROJECT:	"Investigation of Ion Beam Production and Acceleration Using Linear Electron Beams and a Pulse Powered Plasma Focus"

A-1

APRIL 1, 1983 THROUGH MARCH 31, 1984

A. Collective Acceleration and Related Studies

1. Experimental Research

a) Collective Acceleration of Ions from a Laser Produced Plasma.

In these studies, an intense relativistic electron beam (1 MeV, 30 kA, 30 ns) is injected into a laser produced plasma immediately downstream of the beam injection point, and ions are accelerated by the collective fields of the electron beam. The use of the Q-switched ruby laser (0.1-15 J, 15 ns) has allowed the investigation of ions from plasmas one to three orders of magnitude denser than in the previous puff valve ion source experiments, and has provided preionization of the plasma as well. By carefully varying the laser energy and target material, and using time of flight, range/energy, and Thomson spectrometry as diagnostics of the ion energy, we have found an operating regime in which both the accelerated ion energy and current have been increased dramatically. In summary, we have accelerated protons, C, Al, and Fe ions to peak energies in the range 10-20 MeV/amu at current levels in excess of 100 Amperes. Approximately 10% of the injected electron beam energy has been converted to ion energy in these experiments, more than an order of magnitude better than previous results from the puff valve ion source. These results, achieved this past summer, have not yet been

published, although early results and a description of the experiments were published in a paper entitled, "Collective Acceleration of Laser Produced Ions," (IEEE Trans. NS-30, 3186, 1983) enclosed in Appendix A.

b) Collective Acceleration of Ions from a Localized Gas Cloud. This work, which constitutes Linton Floyd's Ph.D. thesis studies (a copy of which will be sent to AFOSR under spearate cover), includes the first collective ion acceleration energy spectra extending to below the injected electron beam energy. A paper detailing these latest results is currently under preparation.

c) "Beam Front Accelerator" Studies. This concept, in which enhanced ion energies are achieved by control of the propagation velocity of the electron beamfront using a helical slow wave structure, has been the subject of considerable effort during the past year. The major result of the work has been the successful control of the beam front velocity using the helical slow wave structure, a result detailed in a paper, "Studies of the Helix Controlled Beam Front Accelerator Concept," (IEEE Trans. NS-30, 3183, 1983) enclosed in Appendix A. Ion acceleration studies, in which we attempt to accelerate ions in the potential well of the beamfront, are currently underway.

d) Beam Propagation Studies. We have conducted two experimental studies of beam propagation in vacuum, one in which radial force balance is achieved by a confining magnetic field, and one in which it is achieved by the charge neutralization provided by positive ions

introduced at the injection point. The major results of these studies are detailed as follows:

i) Intense Electron Beam Propagation in Vacuum in the Presence of an Applied Magnetic Field. These studies were undertaken to determine to what extent actual beam currents observed in laboratory experiments agree with available theory and simulation results. The major results of this study are: 1) At high magnetic fields, the current that can be propagated in a given size drift tube is in good agreement with the space charge limiting value given by Bogdankevich and Rukhadze:

$$I_L = \frac{4\pi\epsilon_o m_o c^3}{e} \frac{(\gamma_o^{2/3} - 1)^{3/2}}{1 + 2 \ln \frac{b}{a}}$$

where b is the tube radius and a is the beam radius, and 2) The maximum current that can be propagated down a given size drift tube occurs at different values of the applied magnetic field in each case but is approximately independent of tube size. This is consistent with the above limiting current for the case a ≈ b. Good agreement with theoretical expectations has been achieved in these studies (see Part 2 of this section), and a paper detailing these studies is currently under preparation.

ii) Intense Beam Propagation through a Localized Plasma into Vacuum. A preliminary study of the propagation of charged particle beam energy into vacuum after passing an intense electron beam through a

localized plasma (from the puff valve or laser ion source) has been conducted. The major results of this study, detailed in a paper, "Electron Beam Propagation through a Localized Plasma into Vacuum," (submitted to Phys. Rev. Lett. for publication and included in Appendix A) include:

(1) Electron beam current well in excess of the space charge limiting value I_L (here about 8 kA assuming the radius of the beam is equal to the current collector radius) can propagate into a vacuum drift tube if a localized source of ions is provided at the injection point.

(2) The propagation of electron beam current to a given axial position is critically dependent upon the peak pressure (and, therefore, the density of ions potentially available for charge neutralization) of the localized gas cloud; this implies that the propagation results from charge neutralization provided by the localized source, rather than from ions drawn off the drift tube walls or from the background vacuum.

(3) The time delay between the arrival of the electron pulse at the collector and the injected current pulse increases with distance as one might expect; at the same time, however, the width of the collector pulse decreases with distance; a fact which indicates to us that the electrons arriving at the collector come from the late part of the injected beam pulse.

(4) The total energy deposited in the downstream collector at 38 cm is about 50% of the injected beam energy and decreases as the axial position of the collector is increased, even when the peak electron current collected remains about the same.

(5) Neutron production seems to correlate reasonably well with effective propagation of the beam current. However, we should note that although effective electron beam propagation is not observed without ion acceleration, effective ion acceleration does not imply effective beam propagation in every case.

In addition, studies at higher plasma density using the laser ion source indicate that in some cases the electron beam transfers its energy into a moving plasma column that may be close to charge and current neutral. These results form the basis for the research we propose to do during the next grant period.

2. Theoretical Research

During the past year, our theoretical efforts concentrated on two areas: (1) numerical studies of ion acceleration from an intense electron beam interacting with a localized neutral gas and (2) the maximum current that can be propagated down a drift tube as a function of applied magnetic field. Each of these areas is summarized below.

a) Numerical Studies of Ion Acceleration. The lastest in a series of studies in this area was presented at the 1982 Plasma Physics

Conference (Ref. 33, Appendix B). The model and initial studies with this numerical code were presented in the Progress Report last year. The geometry and schematic of the CIA model is again shown here in Fig. 1. As pictorially shown in this figure, we insert a charge neutral plasma at a certain rate in the vicinity of the virtual cathode, i.e. the position of peak beam electron density. Though the insertion rate remains constant in this series of studies, we self-consistently move the neutral plasma injection location with the movement of the virtual cathode yet continue neutral plasma injection at all previous locations (at a geometric rate of injection). In Figs. 2 and 3, we have shown phase-space plots of the beam electrons and the plasma ions at various times. The various parameters of this study are given in the figure caption. As seen from the beam electron phase-space plots, the beamfront continually moves away from the anode plane $z = 0$; at $t = 0.2$ ns, the beam front is near 2 mm, and at $t = 1.6$ ns, the beam front is near 13 mm, indicating a beam front velocity of about $\beta_{BF} \simeq .02\text{-}.03$. Also note the increase in beam thermalization behind the beam front as charge neutralization occurs. From the plasma ion phase-space plots, we see a small group of ions accelerated to a velocity $v_i \sim 2.0 \times 10^7$ m/sec equivalent to a proton energy of 2.1 MeV, i.e. four times the beam energy. Also note that this velocity is very near to twice the beam front velocity.

b) Limiting Current as a Function of Applied Magnetic Field. The purpose of these studies is to understand the properties of an electron beam that is propagating along a grounded drift tube immersed in a

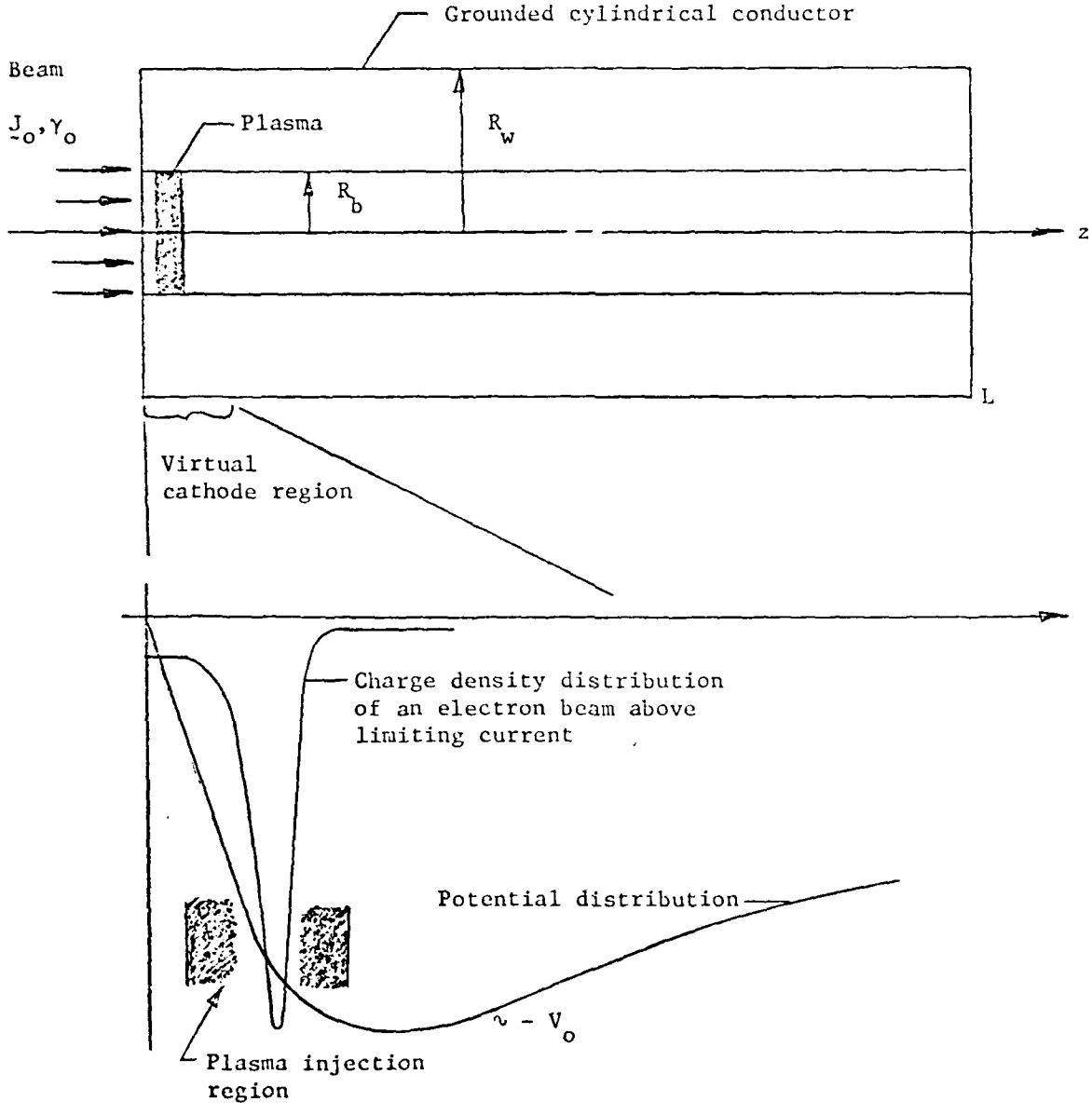

FIG. 1. Geometry and schematic of CIA model.

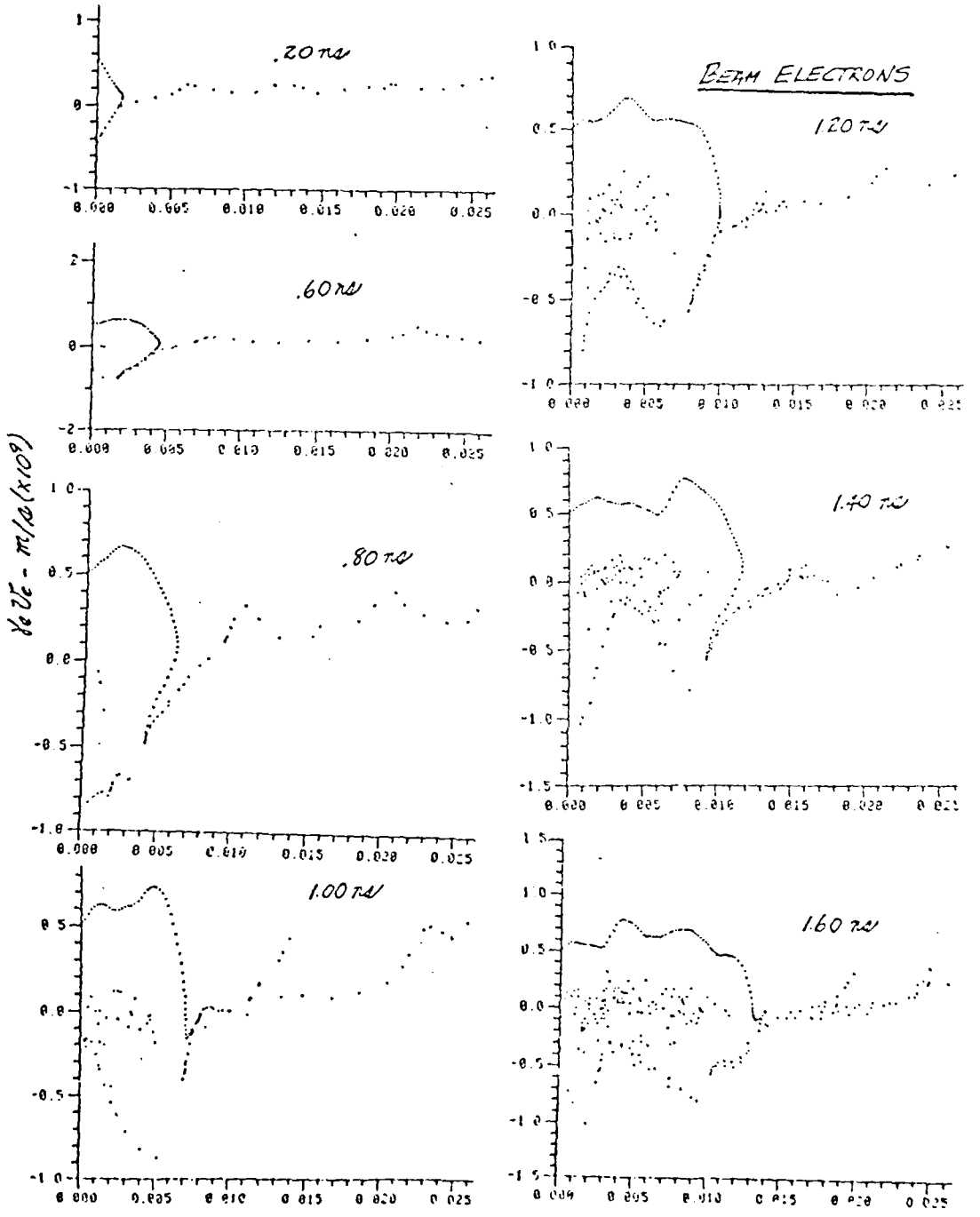

FIG. 2. Phase-space plots of the beam electrons at various times after injection. System parameters (see Fig. 1): R_w = 2 cm, L = 20 cm, I_o = 10 I_L = 20 kA, γ_o = 2, R_b = 0.5 cm. Neutral plasma formation starts at 0.1 ns after the beam is injected and its equivalent constant rate is 630 C/sec. The neutral plasma is placed in a 2 mm window centered about the beam density maximum.

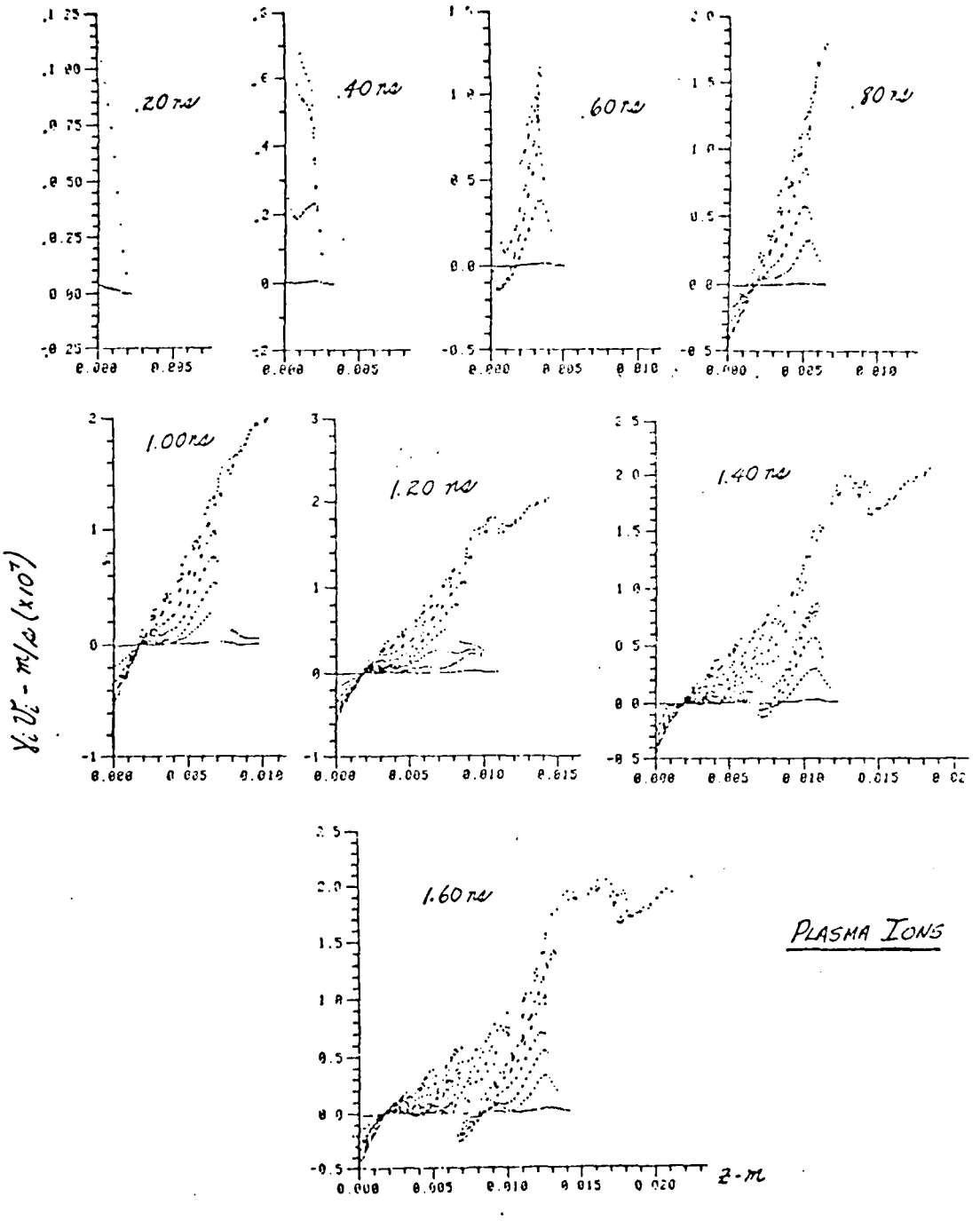

FIG. 3. Phase-space plots of the plasma ions at various times after beam injection. See Fig. 2 for system parameters.

uniform magnetic field. These studies will allow us to estimate the conditions under which the maximum electric field produced by the electron beam occurs. Recall that these conditions are very important for CIA, especially in the helix controlled studies. A very symmetric approach was taken in these studies with the latest results published in IEEE Trans. NS-30, 3183 (1983) and enclosed in Appendix A. In summary, the model can determine the maximum current that can propagate down a drift tube of radius b as a function of applied magnetic field for a solid, uniform density, irrotational, monoenergetic beam of radius a injected through a hole in one end of the drift tube. In the high magnetic field regime, the limit is closely given by the BR limit

$$I_{BR} = \frac{17\ (\gamma_o^{2/3} - 1)^{3/2}}{1 + 2\ \ell n\ \frac{b}{a}}\ kA$$

where $a = R_a$, the injection hole radius. As the magnetic field is lowered, the beam radially expands $a > R_a$, allowing more current to propagate than I_{BR}. This continues until the beam finally fills the drift tube, $a = b$. Further decrease of the applied field from this value sharply reduces the limiting current and finally goes to zero when there is no applied field. The agreement between experiments performed and this model is very good.

B. Compact Pulsed Accelerator

A new concept, "Current Charged Transmission Line with Opening Switch," as a compact pulsed accelerator was invented. A prototype device was constructed and preliminary experiments were carried out. In

this prototype device, the plasma focus was employed as an opening switch and also as a load. The load behaved as a bipolar ion diode in which both the ion beam and electron beam are accelerated in the forward and reverse axial direction, respectively, by the induced pulse voltage. We have demonstrated this principle by measuring the output voltage by a capacitive voltage probe and also by measuring the ion energy. The results of these preliminary experiments are summarized in the following paragraphs and are detailed in three papers enclosed in Appendix A.

1. Ion Beam Generation and Thomson Spectrometer Analysis

Ion beams of various species (H, He, N, Ar, Ne) are produced by the prototype device. The majority of ions produced were found to be of the gaseous elements used for the filling gas. The charge states of ions have been analyzed by a Thomson spectrometer and found to be up to triply ionized in all ion species except H and He ions. By counting the tracks of the Thomson parabolas on the detector, charge state resolved energy spectra were constructed for the ions. The resulting spectra of the different ions species and their charge states are similar to each other.

2. Electron Beam Production Experiment

As expected in the bipolar diode, the ratio of the electron current to the ion current is appproximately $I_e/I_L \tilde{=} (m_i/m_e)^{1/2}$. Thus, the main portion of the output pulse energy is delivered to electron beam energy. A new plasma gun was designed in order to extract the electron

beam in the forward axial direction. Preliminary experimental results show that electron beam currents as high as 10 kA were measured. The heavier fill gases appear to be the most efficient for the purpose of generating a reproducible electron beam. The unstable behavior of the electron beam injected into a gas filled chamber has been photographed using an open shutter camera.

3. Study of Ion Production Efficiency

Total ion flux and energy has been measured with the intention of investigating the efficiency of stored energy conversion into total ion energy. The ion flux is measured with a CR-39 track detector masked by a copper plate which has pinholes at various radial positions. The ion tracks on the CR-39 detector are directly counted with the aid of a scanning electron microscope. The ion energy is inferred from the energy spectra obtained from the Thomson spectrometry. This total ion energy is compared with the stored energy which is directly measured from the main current waveform.

4. Development of New Diagnostics

A Thomson spectrometer of compact size has been developed. The system is calibrated with several different methods which are found to be in good agreement with each other within an error of 2%. A simple magnetic electron anlayzer of the Dembster type has been constructed. The energy of electrons in the range 10 KeV to 1 MeV can be detected by different detectors. Both systems can be used to analyze the ion beams and electron beams from compact pulsed accelerators.

APPENDIX A

Copies of Papers Published during the Period

April 1, 1983 through March 31, 1984

Submitted for publication in Physical Review Letters

ELECTRON BEAM PROPAGATION THROUGH A LOCALIZED PLASMA INTO VACUUM

W. W. Destler, P. G. O'Shea, and M. Reiser

Laboratory for Plasma and Fusion Energy Studies
University of Maryland
College Park, Maryland 20742

The propagation of an intense relativistic electron beam (IREB) through a localized source of ions into a vacuum drift tube has been investigated experimentally. About 70% of the peak injected electron beam current (1 MeV, 27 kA, 30 ns) was found to propagate to a collector 55 cm downstream of the injection point after passing through a hydrogen gas cloud with an effective width of ~ 2 cm. A model is proposed linking electron beam propagation with collective ion acceleration that results in the formation of charge-neutral, current-neutral plasmoids capable of propagation in free space. It is suggested that such processes could play a role in cosmic ray acceleration and laser experiments (high-energy positive ions escaping from target plasma).

The generation and propagation of intense relativistic electron beams (IREB) have been the subject of many theoretical and experimental studies, and the work prior to 1982 is reviewed in the book by R. B. Miller.[1]

With respect to beam propagation, one distinguishes between propagation in (a) vacuum, (b) plasma, and (c) neutral gas, and the beam current I is generally related to the space-charge limiting current I_L in (a), and the Alfvén-Lawson current[2,3] I_A in (b) and (c). Thus, in a vacuum drift tube and in the absence of charge-neutralizing ions, IREB propagation is possible only if $I < I_L$ and if a focusing magnetic field

B is present. The space-charge limiting current then depends on whether both the cathode and the drift tube or only the drift tube are immersed in the magnetic field.[4] In the first case, the assumption that $B \to \infty$ yields the formula for I_L by Bogdankevich and Rukhadze.[5]

For a beam with co-moving ions, as in our experiments, neither I_L nor I_A can be applied. One can, however, derive a general upper limit for the current from power-balance considerations, i.e. from the fact that kinetic energy is spent to build up electromagnetic field energy along the path of propagation.[6] If f_e and f_m define the fractional charge and current neutralization due to positive ions, $(\gamma_o - 1)mc^2$ and $(\gamma_f - 1)mc^2$ the kinetic energy at injection and at the beam front, b/a the ratio of drift tube radius to beam radius, one obtains the following relation for the beam current:

$$I = I_o \frac{(\gamma_o\gamma_f - \gamma_f^2)(\gamma_f^2 - 1)^{1/2}}{[0.25 + \ell n \frac{b}{a}][(1 - f_e)^2\gamma_f^2 + (1 - f_m)^2(\gamma_f^2 - 1)]} , \qquad (1)$$

where $I_o = 4\pi\varepsilon_o mc^3/e = 1.7 \times 10^4$ A for electrons. The limiting current $I = I_P$ due to power balance can be found from the condition $\partial I/\partial\gamma_f = 0$. By setting $f_e = 0$, $f_m = 0$, one obtains the special case $I_P = I_L$.

For beam propagation when $I > I_L$, a plasma or neutral gas is usually provided to achieve charge neutralization by stationary positive ions,[7] and the current is limited by $I < I_P$ (with $f_e = 1$, $f_m = 0$). Propagation into free-space vacuum is possible if co-moving particles of opposite charge are present to assure both charge and current neutralization ($f_e = 1$, $f_m = 1$).

In our present paper, we describe experiments in which IREB

propagation in a vacuum drift tube is achieved with currents $I \gg I_L$ when a source of positive ions is provided at the drift tube entrance. These studies were motivated by observations with collective ion acceleration experiments at our laboratory where an IREB pulse is injected through a localized gas cloud or plasma into a vacuum drift tube.[8] We found that the presence of such an "ion source" at the drift tube entrance not only produced high-energy positive ions by collective acceleration effects, but also facilitated the propagation of a large fraction of the electron beam current down the drift tube.[9] Similar effects were also observed in collective acceleration studies by other groups.[10] To obtain a better understanding of the conditions for beam propagation and of the correlation between propagation and collective ion acceleration, we initiated a systematic experimental investigation, the first results of which are reported below.

The experimental configuration used for the studies is shown in Fig. 1. An IREB (1 MeV, 27 kA, 30 ns FWHM) from a 3 mm diameter tungsten cathode was injected through a 26 mm hole in the stainless steel anode plate (located 6.3 mm from the cathode) into the drift tube region. The drift tube diameter was 15 cm, and the vacuum pressure was in the range 10^{-5}-10^{-4} torr. No focusing magnetic field was used. A well localized hydrogen gas cloud with an effective width of about 2 cm was produced on the downstream side of the anode by firing a fast gas puff valve 540 μs before electron beam injection. By varying the charging voltage of the capacitor bank that powers the puff valve, the effective pressure in the cloud seen by the electron beam could be varied up to a peak pressure of about 100 mTorr. Ionization of the gas

results from electron-impact and ion-avalanche processes.

The current reaching a given position in the drift tube was measured using a low-impedance (14 mohms) current collector with a carbon beam stop 7.4 cm in diameter. Figure 2 shows typical waveforms from the current collector for (a) the injected current at the anode, (b) the current at z = 38 cm from the anode with no gas cloud present, and (c) at z = 38 cm with a gas cloud at optimum pressure present at the anode.

A thermistor embedded in the carbon beam stop was used to measure the temperature rise of the beam stop which yields an estimate of the total beam energy (electrons and ions) propagated to a given axial position in the drift tube. This calorimeter was calibrated by moving the current-collector/calorimeter to a position near the anode hole and measuring simultaneously the injected beam current and voltage waveforms and the temperature rise of the carbon beam stop. With a total deposited beam energy of approximately 1 kJ, the beam stop temperature was increased by 12° C. Thus, each degree of temperature rise recorded results from about 80 J of beam energy deposition.

As an additional diagnostic, a silver activation neutron detector was placed exterior to the drift tube and used to detect neutrons produced by accelerated protons striking the stainless steel drift tube wall.

Figure 3 shows the results obtained from all three diagnostics for beams injected through the localized gas cloud into evacuated drift tubes of axial lengths 38 and 55 cm.

Figure 4 is a photograph of a 20 mil thick copper witness plate

placed 70 cm downstream of the anode and exposed to the beam under conditions where effective beam propagation is observed. The damage pattern results from thermal effects associated with beam energy deposition. The small size and circular symmetry of the witness plate damage pattern are a clear confirmation of the effective beam propagation due to the gas cloud.

The results of our experiments may be summarized as follows:

(1) Electron beam current in excess of the space charge limiting value I_L (here about 8 kA) can propagate into a vacuum drift tube if a localized source of ions is provided at the injection point.

(2) The propagation of electron beam current to a given axial position is critically dependent upon the peak pressure of the gas cloud; this implies that the propagation results from charge neutralization provided by the localized source, rather than from ions drawn off the drift tube walls or from the background vacuum.

(3) The time delay between the arrival of the electron pulse at the collector and the injected current pulse increases with distance while the width of the collector pulse decreases indicating that the electrons arriving at the collector come from the late part of the injected beam pulse.

(4) The total energy deposited in the downstream collector at 38 cm is about 50% of the injected beam energy and decreases as the axial position of the collector is increased, even when the peak electron current collected remains about the same.

(5) Neutron production by accelerated protons seems to correlate reasonably well with effective propagation of the beam current.

These conclusions support a description of the propagation process which we present here as a plausible explanation of the observed phenomena. In this concept, which is based on the model described in Ref. 6, the electron beam enters the drift tube at a current $I > I_L$. Collisional ionization of the gas provides positive ions for charge neutralization and permits the beam to propagate to the edge of the cloud. As the beam enters the vacuum region downstream from the cloud, the space charge forms a "virtual cathode" from which the electrons are reflected back.[9] The high electric fields of the virtual cathode draw ions from the cloud until the electron beam can propagate further into the vacuum drift region. This process may repeat itself until a channel of ionization has been produced stretching from the anode to the collector, at which time the remaining beam electron current at the back end of the pulse may flow through the channel at nearly the speed of light and be collected. Thus, the fraction of the injected current pulse arriving at the collector depends upon the time necessary to establish the channel of ionization. As the axial position of the collector is moved further downstream, this time increases until it becomes equal to the injected current pulse duration. At this point, the current observed at the collector falls to zero.

The dependence of the propagation on the gas pressure can be explained as follows. At low pressures, ions are not available in sufficient number to achieve the partial neutralization required for

efficient propagation. Thus, the beam spreads radially as it propagates, resulting in more current collected at z = 38 cm than at 55 cm, etc. As the injected gas pressure is increased, an optimum value is reached. Beyond this value, more ions than required for radial force balance are available, and the inertia of the excess ions slows the propagation velocity of the ionization channel. As a result, at higher pressures, effective electron beam propagation cannot be achieved as far down the drift tube than is observed under optimum conditions.

The propagation of charged particles in vacuum is of fundamental interest in many areas such as astrophysics, laser fusion, ion propulsion, etc. Alfvén,[2] in one of the first papers on this topic, studied the propagation of relativistic electrons through an interstellar plasma and concluded that the pinch force due to the magnetic self field of the electron stream results in the upper limit $I \leq I_A = I_o \beta\gamma$. In the absence of a charge neutralizing plasma, it is clear from our results and the preceding discussion that propagation requires co-moving positive ions to assure charge and current neutrality. Thus, if an intense flux of relativistic electrons is ejected from an object (e.g. star, laser pellet) into free-space vacuum, the negative space charge forms a "mirror" reflecting the electrons back towards the surface. If a plasma is present, collective acceleration of positive ions facilitates propagation away from the surface. This process is different from ambipolar diffusion in that the relativistic electrons provide the energy source for propagation into vacuum. A large number of reflecting electrons accelerates a smaller number of ions until the electron pulse terminates, or the supply of ions is cut

off, or the co-moving ions at the front of the stream have reached the same velocity as the injected electrons[6] (in which case no further electron reflections occur at the front and a charge and current neutralized "plasmoid" is formed). Thus, collective ion acceleration associated with the propagation of intense electron streams into free space vacuum could play a role in the generation of high-energy cosmic rays whose origin is still an open question.[11]

This mechanism could also explain the energetic positive ions observed in laser-target interaction experiments[12] when the fast electrons produced in the target try to escape from the target-plasma surface. We hope that future results of our investigations will provide further understanding of the correlation between collective ion acceleration and beam propagation in vacuum.[13]

We wish to thank J. D. Lawson for helpful comments and discussions. This work was supported by the Air Force Office of Scientific Research and by the U.S. Department of Energy.

[1]R. B. Miller, An Introduction to the Physics of Intense Charged Particle Beams, (Plenum Press, New York, 1982).

[2]H. Alfvén, Phys. Rev. 55, 425 (1939).

[3]J. D. Lawson, J. Electr. and Contr. 3, 587 (1957); 5, 146 (1958).

[4]M. Reiser, Phys. Fluids 20, 477 (1977).

[5]L. S. Bogdankevich and A. A. Rukhadze, Usp. Fiz. Nauk. 103, 609 (1971) [Sov. Phys.--Usp. 14, 163 (1971)].

[6]M. Reiser, Proc. of the ECFA-RAL Meeting, "The Challenge of ULtra-High

Energies," Oxford 1982, p. 131 (published by Rutherford-Appleton Laboratory, Chilton, Didcot, U.K.)

[7]To our knowledge, the first paper reporting experiments on electron beam propagation in a gas-filled drift tube is that by S. E. Graybill and S. V. Nablo, Appl. Phys. Lett. 8, 18 (1966).

[8]W. W. Destler, L. E. Floyd, and M. Reiser, IEEE Trans. Nucl. Sci. 26, 4177 (1979); Phys. Rev. Lett. 44, 70 (1980); J. T. Cremer and W. W. Destler, IEEE Trans. Nucl. Sci. 30, 3186 (1983).

[9]W. W. Destler, H. S. Uhm, H. Kim, and M. Reiser, J. Appl. Phys. 50, 3015 (1979).

[10]R. Adler, J. A. Nation, and V. Serlin, Phys. Fluids 24, 347 (1981); F. Mako, A. Fisher, N. Rostoker, D. Tzach, IEEE Trans. Nucl. Sci. 26, 4199 (1979).

[11]A recent review on the topic of acceleration of galactic cosmic rays was given by W. I. Axford in, "Origin of Cosmic Rays," edited by G. Setti, G. Spada, and A. W. Wolfendale, D. Reidel Publishing Company, 1981, p. 339-358.

[12]J. S. Pearlman and G. H. Dahlbacka, Appl. Phys. Lett. 31, 414 (1977); Y. Gazit, J. Delettrez, T. C. Bristow, A. Entenberg, and J. Soures, Phys. Rev. Lett. 43, 1943 (1979); G. D. Tsakiris, K. Eidmann, R. Petsch, and R. Sigel, Phys. Rev. Lett. 46, 1202 (1981); H. Hora in Laser Interaction and Related Plasma Phenomena, edited by H. Hora and G. H. Miley (Plenum Press, New York, 1983), Vol. 6.

[13]A more comprehensive description of our work, including experiments with laser-produced plasmas, will be published in a separate paper.

FIG. 1. Experimental configuration for the beam propagation studies with the puff valve ion source at the anode.

FIG. 2. Current collector waveforms for (a) injected current, (b) current at z = 38 cm with no gas injected, and (c) current at z = 38 cm with optimized gas cloud pressure at injection.

FIG. 3. Results of a) current collector, b) calorimeter, and c) neutron detector measurements at z = 38 cm and z = 54.6 cm as a function of gas cloud peak pressure at time of beam injection (Δp = 50 - p_{max} ≈ 50 mTorr).

FIG. 4. Photograph of copper witness plate at z = 70 cm with optimized gas cloud pressure at injection.

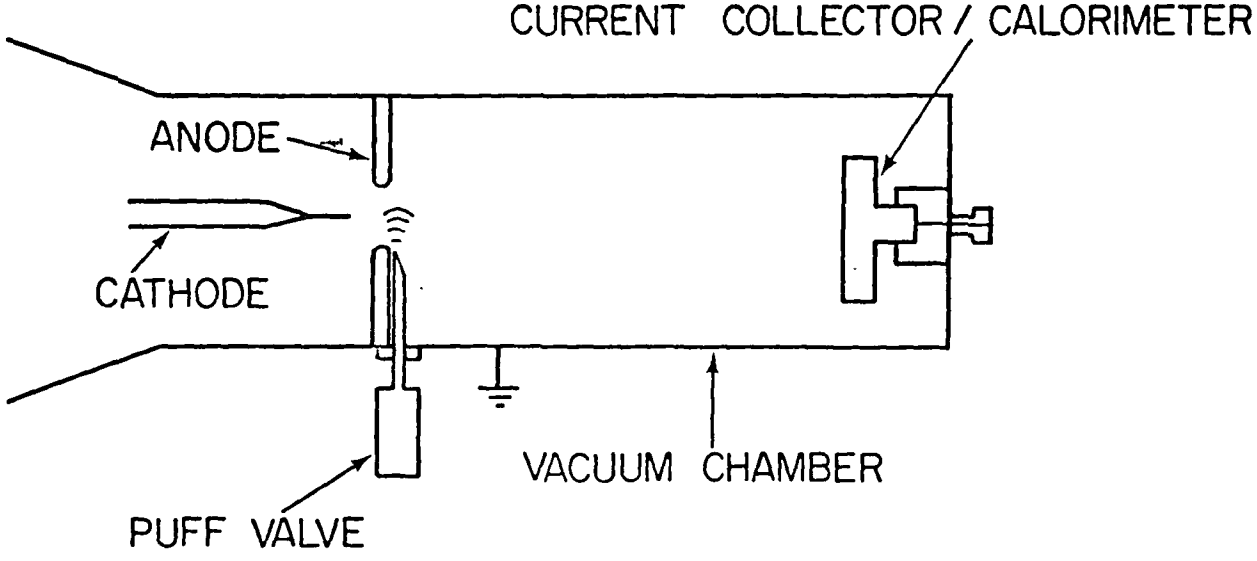
CURRENT COLLECTOR / CALORIMETER
ANODE
CATHODE
VACUUM CHAMBER
PUFF VALVE

FIG. 1

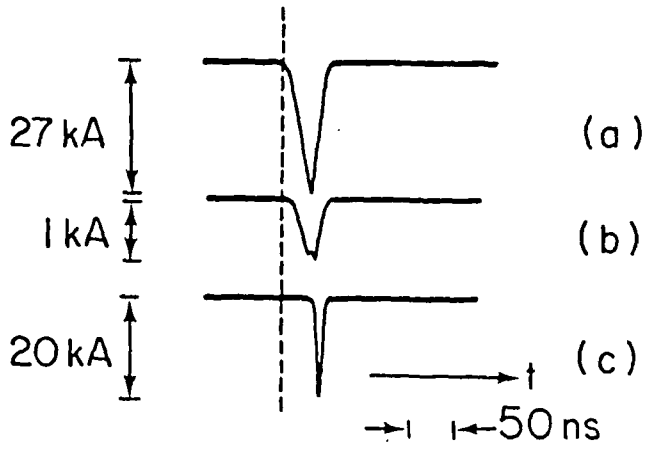

FIG. 2

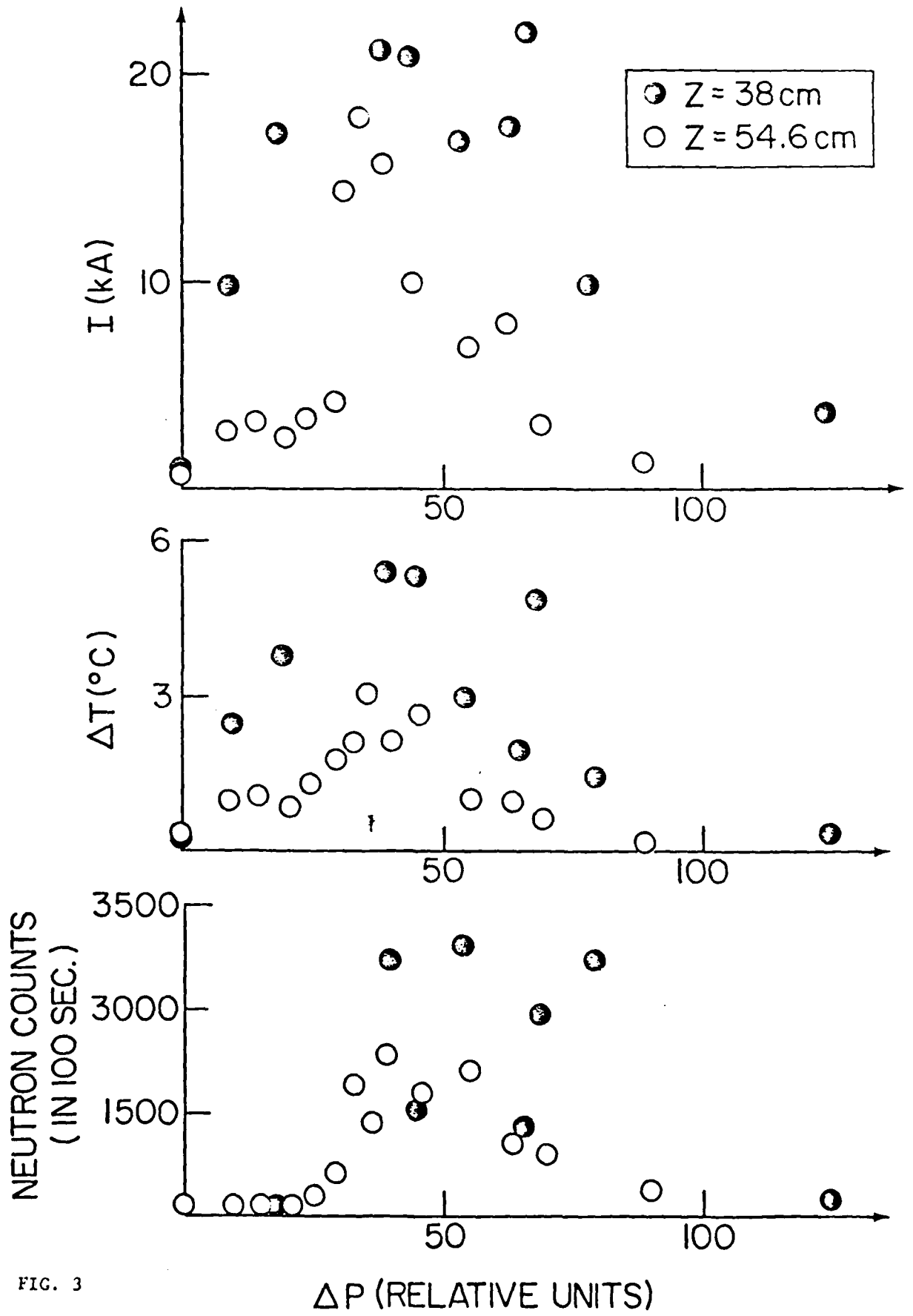
Z = 38 cm
Z = 54.6 cm
I (kA)
20
10
50
100
ΔT (°C)
6
3
50
100
NEUTRON COUNTS
(IN 100 SEC.)
3500
3000
1500
50
100
ΔP (RELATIVE UNITS)

FIG. 3

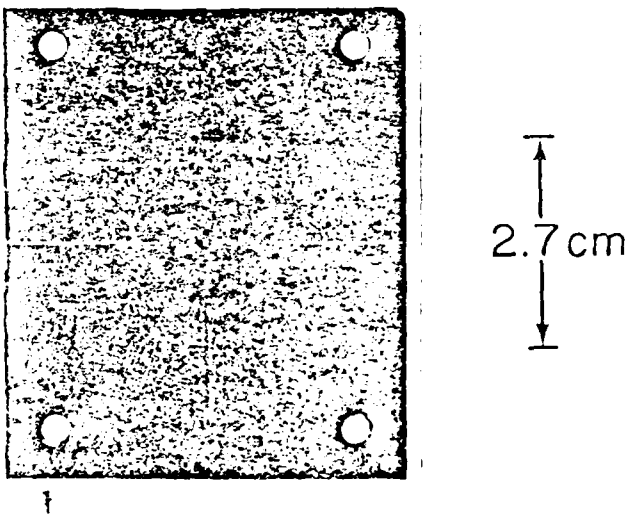

FIG. 4

COLLECTIVE ACCELERATION OF LASER PRODUCED IONS*

J. T. Cremer and W. W. Destler

Electrical Engineering Department
University of Maryland
College Park, Maryland 20742

Summary

Experimental studies of the collective acceleration of laser produced ions have been conducted. An intense relativistic electron beam (1 MeV, 30 kA, 30 ns) is emitted from a 4 mm diameter tungsten cathode and passes through a 2.4 cm hole in a stainless steel anode into a 14 cm diameter downstream drift tube. Ions are provided on the downstream side of the anode plane by firing a 4-10 J, 15 ns Q-switched ruby laser pulse at solid or foil targets mounted on the downstream side of the anode plane. Accelerated ion energies are measured using time of flight and range energy/track etching techniques. Ion charge states are measured using an E*B Thomson spectrometer. Results will be compared with measurements of the pre-acceleration characteristics of the laser produced ions from these target geometries obtained using an electrostatic analyzer.

Introduction

Studies of the collective acceleration of ions from an independently controllable ion source using an intense linear electron beam have been conducted in our laboratory at the University of Maryland for the past several years.[1-6] This work was a natural outgrowth of early experiments by Graybill, et al[7] and Luce[8] who initially investigated collective acceleration in the gas-filled and evacuated drift tube geometries, respectively. This early work was followed by experimental and theoretical investigation of this phenomena at several other laboratories,[9-13] as well as our own. During this period, we have reported the acceleration of a large number of ion species from puff-valve and laser-target ion sources to peak energies of about 5 MeV/amu independent of the ion mass. In these experiments, the electron beam pulse was 1-1.5 MeV, 30 kA, 30 ns FWHM. Protons have been accelerated to energies of 16-20 MeV in related experiments.

Initial experiments[4] of the collective acceleration of laser produced ions reported by our group indicated that although laser preionization did not result in higher peak ion energies, it did appear to increase the number of ions that are accelerated to high energy (3-5 MeV/amu). For this reason, we have initiated a systematic study of this configuration in which the characteristics of the laser-produced plasma from different target configurations have been measured using an electrostatic analyzer. The ion energies and charge states of the preacceleration plasma can then be compared to those measured after collective acceleration occurs.

Studies of Laser Produced Plasmas from Solid and Foil Metallic Targets

A comparative study of laser produced ions from solid and foil metallic targets has been performed in which an electrostatic analyzer and biased charge collectors were used as diagnostics. The experimental configuration is shown in Fig. 1. A Q-switched, 4-10 J, 15 ns ruby laser is focused to 10^{11} W/cm^2 on solid Al, Fe, and Ta targets and on .0003" Al foil, .0004" Fe foil, and .0002" Ta foil targets for various angle pairs (θ_i, θ_d), where θ_i is the angle of laser incidence and θ_d is the angle of ion detection. Data has been obtained for angle pairs with respect to the target normal of (5°,0°), (40°,45°), (0°,45°), (45°,0°), (22.5°,22.5°) and (180°,0°). The relative ion charge state distribution is measured using a 127° electrostatic analyzer located about 2 m from the target. In the analyzer detector, ions produce secondary electrons when they strike an aluminum knob biased to -20 kV, and the secondary electrons are accelerated onto NE102 scintillant, where the light produced is detected using a photomultiplier tube. A typical result of these studies is shown in Fig. 2, where the relative ion number for each charge state is plotted as a function of ion energy. It is easily seen that for the solid aluminum target results shown, the ion population is predominantly in charge states 1-3, with a maximum charge state observed of 5. An indication of the actual ion current has been obtained using biased charge collectors located 20 cm from the target. The current collected, if assumed to be in the same charge state distribution as that measured by the electrostatic analyzer, can be used to obtain a rough estimate of the total ion number. For this particular case, it is estimated that about 10^{14} Al ions are produced from the target on each shot.

It is interesting to compare this number with the total number of atoms vaporized by the laser as obtained from measurements of the volume of the pit in the solid produced by the laser. For this case, such measurements show that about 10^{19} atoms are liberated from the surface of the solid, an indication that only a small fraction of these atoms are ionized.

The complete results of this survey are too extensive to be detailed here. The main conclusions of the study are as follows: 1) The highest charge states and ion currents are observed when $\theta_i = 0°$ and $0° < \theta_i < 45°$ for all targets, 2) Solid targets deliver substantially more ion current at all charge states than do thin foil targets, and 3) The highest charge states observed are $Z = 6$ for aluminum and $Z = 5$ for iron and tantalum.

Collective Acceleration of Laser Produced Ions

The general experimental configuration used for these studies is shown in Fig. 3. An intense relativistic electron beam (1 MeV, 30 kA, 30 ns FWHM) is emitted from a 4 mm diameter cold tungsten cathode. The anode, a 6 mm thick stainless steel plate, has a 24 mm diameter hole on axis through which the beam passes into the downstream drift region. The diameter of the downstream drift tube is 14 cm. Ions to be accelerated are provided by firing a 4-10 J, 15 ns Q-switched ruby laser at solid or foil targets mounted in the downstream drift region. The timing of the laser firing must be adjusted such that ions are produced before electron beam injection, but not so early as to short the diode. In these experiments, a laser-electron beam firing delay of 0.5 microseconds was found to be optimum. Accelerated ions are usually not observed when the laser is not fired.

* Work supported by the Air Force Office of Scientific Research and the U.S. Department of Energy

0018-9499/83/0800-3186$01.00 ©1983 IEEE

Effect of Target Geometry.

A variety of different target geometries were tested, including 1) Foil targets stretched across the anode hole and irradiated on axis by the laser just before electron beam injection, 3) Wire targets (1 mil diameter) stretched across the anode hole in a similar fashion, 3) Rods (62 mil diameter) installed in a manner similar to the wire, and 4) Solid targets mounted off axis on the downstream side of the anode plane, as shown in Fig. 3. A typical ion time of flight measurement is shown in Fig. 4. In this case, the ion time of flight between two charge collection probes 30 cm apart is measured after any accompanying electrons are swept away using a transverse magnetic field. The photograph shown is for an off-axis aluminum solid target, and indicates a peak velocity of about 0.1 c, or about 5 MeV/amu. The peak ion energies obtained in this manner for the various target geometries are shown in Fig. 5. It is interesting to note that all of the configurations that potentially perturb the electron flow through the anode hole (wire, rod, and foil targets) resulted in lower peak accelerated ion energies than did the off-axis targets. All subsequent measurements have been performed with off-axis targets.

Charge State Measurements

Accelerated ion charge states were measured using a Thomson E1B spectrometer (see Fig. 3) similar to that designed by M. J. Rhee.[14] The ion beam is first collimated by two 0.3 mm pinholes separated by 23 cm. A magnetic field transverse to the collimated beam is provided by a permanent magnet and two pole pieces located inside the drift chamber. An insulated conducting plate located on the inside surface of one pole piece is connected to a high voltage power supply to provide an electric field parallel to the magnetic field. Typical values for E and B are 6 x 10^5 V/m and 0.15 T, respectively. Ions deflected by these fields are detected by a CR-39 track plate located 2.1 cm downstream of the pole pieces. The ion tracks become visible under a microscope after the exposed plate is etched in an NaOH solution.

Ions of a given charge to mass ratio Z/A and varying energy trace out a parabola on the track plate given theoretically by

$$x = \frac{5.2 \times 10^{-9} E_x [(L_1^E)^2 + 2L_1^E L_2^E)] y^2}{\frac{Z}{A}\left[\int_0^{L_1^B}\int_0^z B_x(z)\,dz\,dz\right]^2} \text{ (meters)}$$

where x is the coordinate in the direction of E and B (and therefore the direction of electric field deflection) and y is the direction of magnetic field deflection. The distance L_1^E over which the electric field is applied is assumed to be equal to the pole piece axial length. The post electric field drift distance to the track plate is L_2^E, and L_1^B is the distance over which the magnetic field is applied (in this case $L_2^B = 0$).

Fig. 6 is a photograph of a typical track plate. The coordinate axes and origin are obtained by setting either E_x or B_x to zero, or both, and accelerating ions in the normal fashion. The results of these measurements are summarized in Table I. It is easily seen that the highest charge state observed increases with ion mass. Peak energies determined from these measurements were in the range 1-2 MeV/amu, although Thomson spectrometry is not a particularly good diagnostic for determining ion energy, since resolution is poorest at high energy. This lower peak ion energy is attributable to the fact that the beam energy was about 1 MeV in this case, as compared to about 1.5 MeV in the time of flight measurements of ion energy.

In contrast to previous studies of the collective acceleration of ions from a localized gas cloud,[3-9] impurity contamination (particularly by protons) of the accelerated ion beam is a common occurrence. This contamination can be reduced, but not eliminated, by firing the laser at the target to clean the surface immediately before a shot. The results for tantalum and iron are diffcult to interpret, because the resolution of the spectrometer is not good enough to resolve individual charge states. In addition, tantalum has a high adsorption coefficient, and proton (and possibly nitrogen) contamination of the ion beam is routinely observed. When accelerated protons are observed, however, they are accelerated to approximately the same peak velocity as the fastest heavy ions. In the previous studies of the collective acceleration of ions from a localized gas cloud, it was also observed that all charge states were accelerated to approximately the same peak velocity.[6] Within experimental error, this appears to be the case in this work as well. These results appear to imply that the acceleration process is not electrostatic, in which case higher charge state ions should reach higher energies, but more likely the result of a moving potential well acceleration process similar to that used by Olson to describe ion acceleration in the gas filled geometry.[9]

Range-energy measurements of the accelerated ion energy are consistent with those obtained from the ion time of flight measurements, except when protons are present as contaminants in significant numbers (e.g. for Ta). This is a result of the fact that in this energy regime, the proton range is much greater than the heavy ion range for the same energy/nucleon.

References

1. W. W. Destler, L. Floyd, and M. Reiser, IEEE Trans. Nucl. Sci. 26, 4177 (1979).
2. W. W. Destler, L. E. Floyd, and M. Reiser, Phys. Rev. Lett. 44, 70 (1980).
3. L. E. Floyd, W. W. Destler, M. Reiser, and H. M. Shin, J. Appl. Phys. 52, 693 (1981).
4. W. W. Destler, L. E. Floyd, J. T. Cremer, C. R. Parsons, M. Reiser, and J. W. Rudman, IEEE Trans. Nucl. Sci. 28, 3404 (1981).
5. W. W. Destler and J. T. Cremer, J. Appl. Phys. 54, 636 (1983).
6. W. W. Destler, Rev. Sci. Inst. 54, 253 (1983).
7. S. Graybill and J. Uglum, J. Appl. Phys. 41, 236 (1970).
8. J. S. Luce, Ann. N. Y. Acad. Sci. 20, 336 (1973).
9. C. L. Olson and U. Schumacher, in Springer Tracts in Modern Physics: Collective Ion Acceleration, edited by G. Hohler (Springer, New York, 1979), Vol. 84.
10. J. A. Nation, G. Providakes, and V. Serlin, in Proceedings of the Fourth International Topical Conference on High Power Electron and Ion Beam Reserach and Technology, Palaiseau, France, 1981, p. 667.
11. L. S. Bogdankevich I. L. Zhelvazkov, and A. A. Rukhadze, Sov. Phys, JETP 30, 174 (1970).
12. M. Masuzaki, Y. Tamagawa, K. Kamada, S. Watanabe, S. Kawasaki, Y. Kubota, and T. Nakanishi, Jpn. J. Appl. Phys. 21, L326 (1982).
13. J. W. Poukey and N. Rostoker, Plasma Phys. 13, 897 (1971).
14. M. J. Rhee, IEEE Trans. Nucl. Sci. 28, 2663 (1981).

TABLE I. Results of charge state measurements.

Target Material	Z_{max}/A	$W_{max}(\frac{MeV}{amu})$	*Observed* Impurities
Carbon	5/12	~ 2	H^+
Aluminum	10/27	~ 1	H^+
Iron	~ 15/56	~ 1.5	H^+, H_2^+
Tantalum	~ 45/181	~ 1	H^+

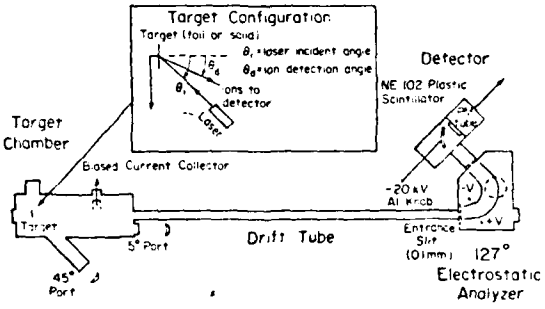

FIG. 1 Experimental configuration for studies of laser produced ions from solid and foil metallic targets.

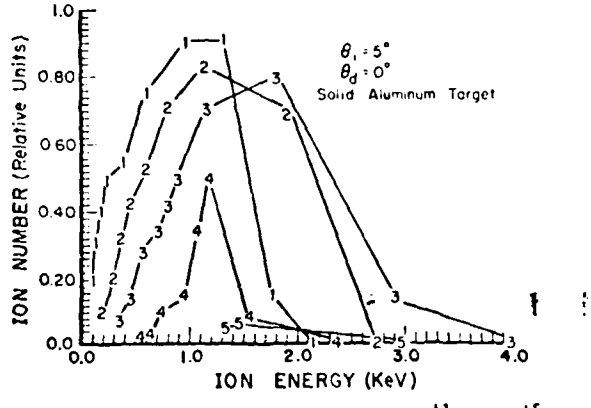

FIG. 2 Typical ion energy spectra for Al^{+1} to Al^{+5} as observed with the electrostatic analyzer.

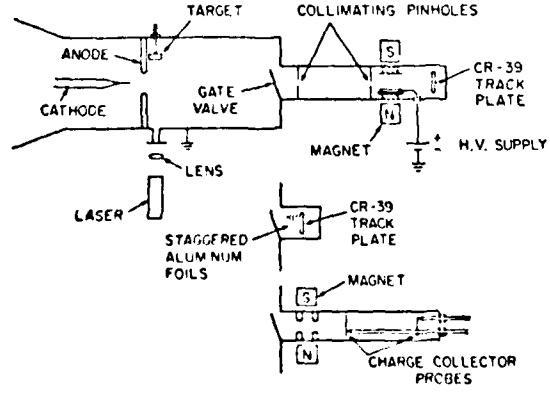

FIG. 3. Experimental configuration for studies of the collective acceleration of laser produced ions.

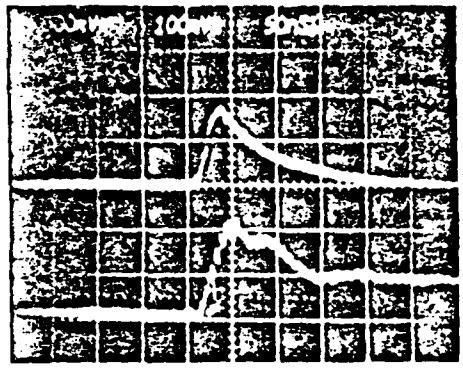

FIG. 4. Typical ion current waveforms from ion time of flight studies. Top trace--front probe, 3 A/division, bottom trace--back probe (30 cm downstream), 0.1 A/division.

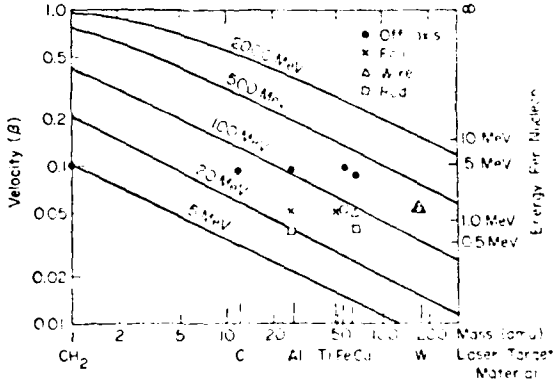

FIG. 5. Peak ion velocity for various target geometries and materials.

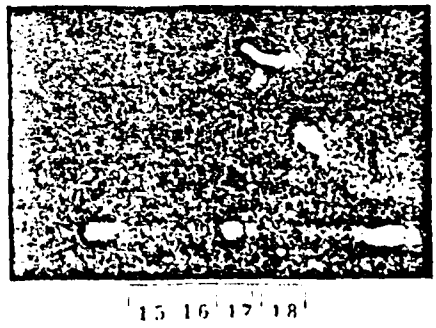

FIG. 6 Microscope photograph of typical Thomson spectrometer track plate for carbon ions. Each small division corresponds to 0.1 mm.

STUDIES OF THE HELIX CONTROLLED BEAM FRONT ACCELERATOR CONCEPT*

W. W. Destler, P. G. O'Shea, M. Reiser, C. D. Striffler, D. Welsh, and H. H. Fleischmann†

Electrical Engineering and Physics Departments
University of Maryland
College Park, Maryland 20742

†On leave from Cornell University, Ithaca, New York, 14850

Summary

Helix controlled collective ion acceleration involves the use of a helical slow wave structure to control the propagation velocity of an intense relativistic electron beam front, in which ions could be trapped and accelerated to high energy. Experimental and theoretical studies of the propagation of an IREB inside both cylindrical and helical conducting boundary systems have been conducted. In the experiments, an IREB (1 MeV, 30 kA, 30 ns, confined by an applied axial magnetic field) is injected from a 1 cm diameter hollow stainless steel cathode through a 2.4 cm diameter hole in a stainless steel anode into either cylindrical or helical downstream drift chambers. Beam propagation in the cylindrical systems is in good qualitative agreement with theoretical calculations based on a modified Bogdankevich, Rukhadze beam model.[3] When a helical slow wave structure is used as the conducting boundary, the beam front velocity is significantly reduced to values approaching those associated with the helix pitch angle.

I. Introduction

The Helix Controlled Beam Front Accelerator[1,2] a concept first proposed by H. Kim, involves the use of a helical slow wave structure to control the propagation velocity of an intense relativistic electron beamfront. Positive ions can then be trapped in the space charge potential well at the beamfront and accelerated to high energy by varying the helix pitch angle along its length. The concept is dependent upon the fact that the maximum electron current that can propagate in a grounded cylindrical drift tube is limited to values less than or equal to the space charge limiting current, given approximately by

$$I_L = \frac{17{,}000(\gamma_o^{2/3} - 1)^{3/2}}{(1 + 2\ln\frac{R_w}{R_b})(1 - f)} \text{ [A]} \qquad (1)$$

where γ_o is the relativistic mass factor of the injected electrons, R_w is the tube radius, R_b is the beam radius, and f is the fractional neutralization, if any, provided by ions.[3] If the tube is initially charged to a negative potential V_o, the electron energy will be reduced to a value given by $\gamma = \gamma_o - eV_o/mc^2$, thus reducing the limiting current substantially. An electron beam with $I < I_L$ in the unbiased drift tube could be effectively prevented from propagating in the biased tube by this effect. If the input end of the biased tube were then shorted to ground, a grounding wave would propagate along the cylinder at the phase velocity of transmission line waves in such a system. For a simple cylindrical boundary system, this velocity would be c. For a helical slow wave structure of radius a inside of an outer conducting boundary of radius b, this velocity is given at low frequencies by

$$v_{ph} = \frac{c\sin(\psi)}{[1 + (\frac{1 - a^2/b^2}{2\ln b/a} - 1)\cos^2\psi]^{1/2}} \qquad (2)$$

and at high frequencies by $v_{ph} = c\sin(\psi)$ where ψ is the helix pitch angle. In this manner, the propagation velocity of the electron beam front could be controlled by varying the helix pitch along its length.

In experiments to date, the initial charging of the helix has been accomplished by the early part of the electron beam pulse. The grounding of the input end of the helix was accomplished by surface breakdown across an insulating support. The pitch of the helix was chosen to match the ion velocity readily obtained in such systems without the helix. For a 1 MeV electron beam a helix pitch in the range 0.05-0.1 was used,[2] and an enhancement of the accelerated ion energy over that achieved without a helical slow wave structure of a factor of two was achieved. In this paper, we report a systematic study of the electron beam propagation characteristics in both cylindrical and helical conducting boundary systems as a function of applied magnetic field.

II. Experiments

The general experimental configuration is shown in Fig. 1. An intense relativistic electron beam (1 MeV, 30 kA, 30 ns FWHM) is emitted from a 1 cm diameter hollow stainless steel cathode 1.2 cm upstream of a stainless steel anode plate. A 2.4 cm diameter hole in the anode allows virtually all of the electron beam current to pass into the downstream drift tube. An axial magnetic guide field constrains the radial motion of the beam electrons over the entire experimental length. The current reaching the end of the drift tube is measured using a low impedance Faraday cup.

Beam Propagation in Cylindrical Drift Tubes. The peak electron beam current measured at the downstream end of the drift tube using the Faraday cup is plotted as a function of applied magnetic field for two different diameter drift tubes (grounded at the input end) in Fig. 2. Two important features are apparent from these results: 1) The maximum current that can be propagated is independent of tube radius , and 2) The propagated current at high magnetic fields is greater for the 3.8 cm diameter tube than for the 9.8 cm diameter tube. Both of these results are in qualitative agreement with theoretical expectations.

Beam Propagation in Helical Slow Wave Structures. The peak propagated current measured at the downstream end of two different 3.8 cm diameter helical slow wave structures (grounded at the input end) mounted coaxially inside a 9.8 cm diameter outer cylindrical boundary is also plotted in Fig. 2. This data is for the case where the helix chirality (sense of helix winding) is such that the return current flowing in the helix produces an axial magnetic field in the same direction as that of the applied field. When the helix is wound with opposite chirality, much higher magnetic fields must be applied to achieve effective beam propagation. This result is consistent with the calculated transmission line impedance of about 600 ohms for the .07 pitch helix system and about 300 ohms average for the .1 + .27 pitch helix system, indicating that if the helices are charged up to a sizable fraction of the beam energy, the return current would be several kiloamperes, producing a large axial magnetic field, which may enhance or

*Work supported by the Air Force Office of Scientific Research and The Department of Energy.

0018-9499/83/0800-3183$01.00 ©1983 IEEE

detract from the applied magnetic field. The propagated current is virtually unchanged when the input end is floated, perhaps because inductive isolation after the first few turns allows effective charging of the helix even when the input end is grounded.

The arrival time of the peak electron beam current propagating in helix systems at the Faraday cup relative to that obtained in a cylindrical drift tube of the same diameter is plotted vs. applied magnetic field in Fig. 3. It is easily seen that substantial delays in the arrival time of the peak beam current are only observed for applied magnetic fields in the range 3-6 kilogauss, a result consistent with the expectation that both helix charging and beam-helix interaction should be maximized when the beam current flows near the helix wall.

An attempt to measure the beamfront velocity optically has been made using the configuration shown in Fig. 1. Plastic scintillant (NE102) was placed along the outside of the helix as shown, and light emitted when electrons struck the scintillant was picked up by fiber optic transmission lines. The light pipes were then aligned vertically in order of their axial position and the light observed was photographed using an image converter camera operating in the streak mode. Typical results obtained for both a fast and slow helix are shown in Fig. 4. These results show a beam front velocity of about 0.08 c for the .07 pitch helix and about .3 c for the .1 + .27 pitch helix. Both of these examples are for the case where the helix chirality was such that the return current in the helix produced a magnetic field that reduced the applied magnetic field behind the beam front. In this case, there is reason to believe that substantial beam current would strike the scintillant behind the beamfront. In the case where the helix field added to the applied field, the photographs are much more difficult to interpret, perhaps because electrons do not reach the scintillant as effectively.

III. Model of Solid Beam Equilibrium

To calculate the properties of an intense relativistic electron beam as a function of applied magnetic field and acceleration potential, we consider the system shown in Fig. 5. Our analysis assumes the beam expands adiabatically to a radius R_b where a laminar flow equilibrium is obtained far from the end walls. More specifically, a solid, uniform density electron beam of radius R_a is injected into a long, hollow, grounded drift tube of radius R_w. The entire system is immersed in a uniform axial magnetic field B_{AZ}. The injected beam is irrotational and monoenergetic with energy $mc^2(\gamma_o - 1) = eV_o$. The downstream beam properties shown in Fig. 5, ρ_b, V_ϕ, V_z, E_{sr}, $B_{s\phi}$, and B_{sz} along with the above assumptions are interrelated by:

Conservation of Particle Energy

$$\gamma(r) = \gamma_o + \frac{e}{mc^2}\phi(r) = \frac{1}{\sqrt{1 - \beta_\phi^2(r) - \beta_z^2(r)}}, \qquad (3)$$

where $\beta_\phi = V_\phi/c$, $\beta_z = V_z/c$, and $\phi(r)$ is the electric potential;

Conservation of Canonical Angular Momentum

$$-\frac{eB_{AZ}r_a^2}{2} = r\left[m\gamma(r)V_\phi(r) - eA_\phi(r)\right], \qquad (4)$$

where $A_\phi(r)$ is the downstream vector potential and r_a is the particles' radial position at the anode; and

Radial Force Balance

$$m\gamma(r)V_\phi^2(r)/r = e\left[E_{sr}(r) + V_\phi(r)\left[B_{AZ} + B_{sz}(r)\right] - V_z(r)B_{s\phi}(r)\right]. \qquad (5)$$

To solve the above equations, we assume the downstream charge density $\rho_b(r)$ is constant, i.e., $\rho_b(r) = \rho_b$, and $0 \le r \le R_b$. Then, the assumption of laminar flow implies the relative radial position of an electron in the beam is constant regardless of beam radius, i.e., $r/r_a = R_b/R_a$. Because E_{sr} is linear in r, we assume the azimuthal velocity is of the form $V_\phi = kr$. In addition, assuming $V_z(r)$ is relatively constant in r, B_{sz} can be calculated by finding an $\bar{r}$ such that $B_{sz}(\bar{r}) = \bar{V}_z = V_z(r)$. With the further assumption that all self magnetic fields are contained inside the conducting wall, we can calculate all self fields and potentials. Thus, knowing R_a, R_w, γ_o, and B_{AZ} and choosing the downstream beam radius R_b, we can then calculate the other equilibrium properties, ρ_b, $V_z(r)$, $V_\phi(r)$ via Eqs. (3)-(5). This procedure is iterated until the correct $\bar{r}$ is found. Finally, the total beam current is calculated by $I = \pi R_b^2 \rho_b V_z(\bar{r})$, which in steady state must equal the injected beam current.

Calculated beam properties are shown in Fig. 6 for the case $R_a = 1.0$ cm, $R_w = 4.8$ cm and $\gamma_o = 3.0$. These results show the variation of beam current with beam radius, externally applied magnetic field, and beam density. The beam density is expressed as the potential depression on axis divided by the acceleration voltage. We find that $\bar{r} = 0.5\ R_b$ gives the best fit. In the limit of B_{AZ} approaching infinity and when $\bar{r} = 0$, our results reduce to the Bogdankevich-Rukhadze curve with the limiting current given in Eq. (1) with $f = 0$. The calculations show our assumptions of $V_\phi(r)$ being linear in r and $V_z(r)$ being constant are quite good.

To interpret Fig. 6, select a magnetic field strength and follow that line until the injection current is reached, the beam radius equals the drift tube radius, or the beam becomes unstable. The current limit when the beam becomes unstable is due to loss of radial force balance occurring near the beam axis. On our curves, this region occurs at potential depths beyond the maximum current that can propagate for a given beam radius. If more current is injected than the system allows, the excess current is lost to the walls. For example, if $B_{AZ} = 1$ kG, 10.5 kA would propagate as a 3.6 cm beam, but a 20 kA injected beam would propagate as a 4.8 cm beam with only 17.25 kA. However, at $B_{AZ} = 1.5$ kG, a 4.8 cm beam will not propagate regardless of injection current; the largest beam at 1.5 kG is 3.6 cm at 12.5 kA current.

The above interpretation leads to Fig. 7 which compares theoretical predictions to experimental results. We have plotted maximum beam current vs. applied magnetic field for two wall radii, 4.8 cm and 1.9 cm. Experimental results, points "0" and "Δ," for these two cases are also displayed. When the applied magnetic field is relatively low, the beam current is limited, because the beam fills the tube. At higher magnetic field strengths, the beam current is limited by beam density, because electrons near the beam axis have large potential energies but insufficient kinetic energy to create the V×B forces which keep them in equilibrium. In this magnetic field regime, a virtual cathode forms if the injected current is above the steady state limit plotted. Though there is fairly good agreement between the solid beam model and the experimental data, we clearly need a less restrictive model.

References

1. C. N. Boyer, W. W. Destler, and H. Kim, IEEE Trans. Nucl. Sci. 24, 1625 (1977).
2. W. W. Destler, H. Kim, G. T. Zorn, and R. F. Hoeberling, in Collective Methods of Acceleration (N. Rostoker and M. Reiser, Eds.) Harwood Acad. Pub., 509 (1979).
3. L. S. Bogdankevich and A. A. Rukhadze, Sov. Phys. 14, 163 (1971).

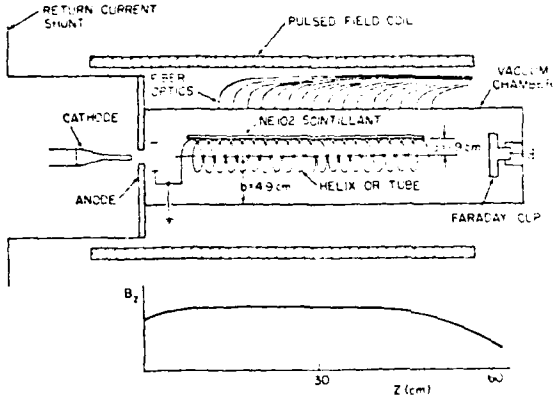

FIG. 1 General Expérimental Configuration.

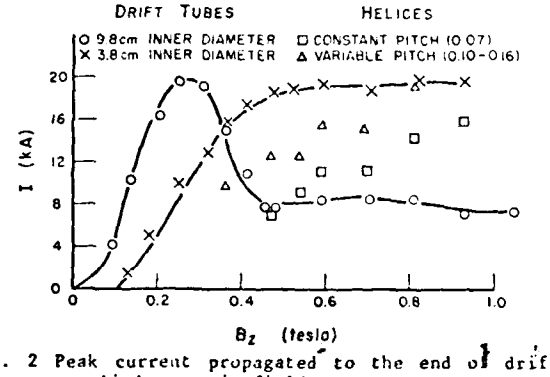

FIG. 2 Peak current propagated to the end of drift tube vs. applied magnetic field.

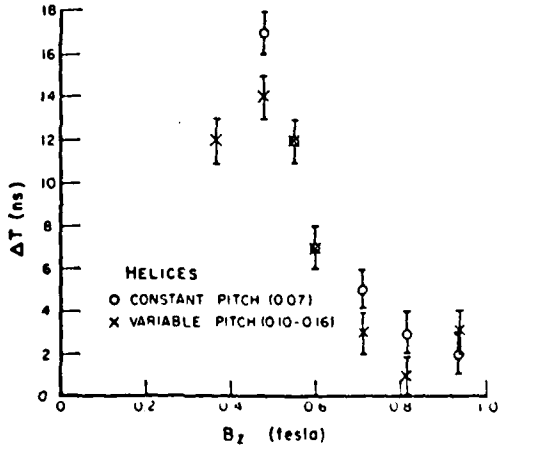

FIG. 3 Arrival time of peak current at Faraday cup vs. applied magnetic field relative to that obtained in a simple cylinder.

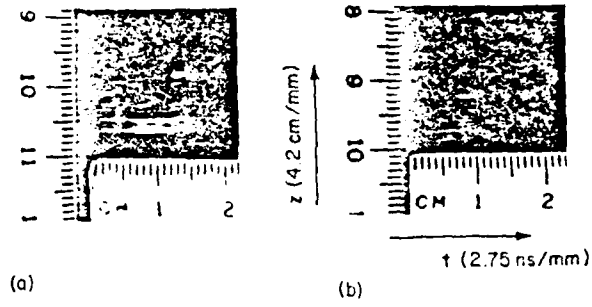

FIG. 4 Streak photographs of beamfront propagation velocity. a) .1 + .27 pitch helix, b) .07 pitch helix.

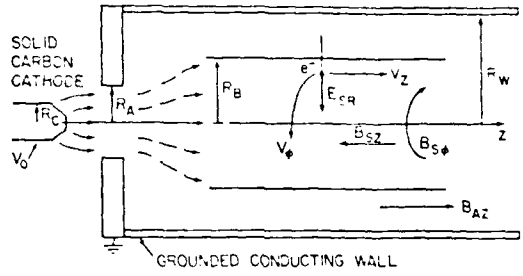

FIG. 5 Schematic of beam model.

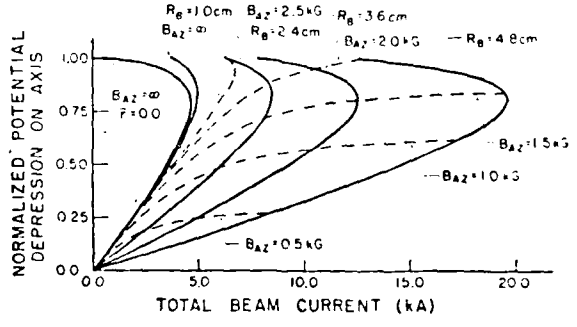

FIG. 6 Downstream beam properties for R_a = 1.0 cm, R_w = 4.8 cm, and γ_o = 3.0. Normalized potential depression on axis vs. axial current with beam radius R_b and applied magnetic field B_{AZ} as parameters.

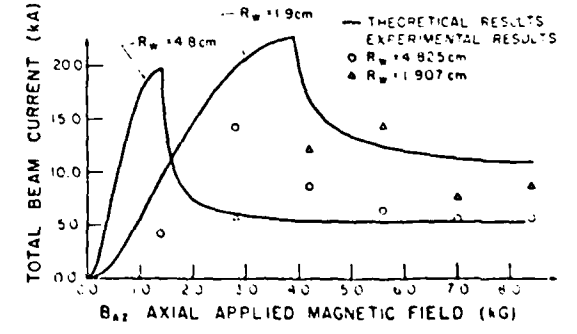

FIG. 7 Maximum beam current vs. applied magnetic field. Comparison of theoretical and experimental results for R_w = 4.8 and 1.9 cm.

BEAM FRONT ACCELERATORS

M. Reiser
University of Maryland, College Park, MD, USA*

(Invited paper presented at the EPAC Meeting "The Challenge of Ultra-High Energies" Oxford, September 27-30, 1982)

ABSTRACT

An intense relativistic electron beam cannot propagate in a metal drift tube when the current exceeds the space charge limit. Very high charge density and electric field gradients (10^2 to 10^3 MV/m) develop at the beam front and the electrons are reflected. When a neutral gas or a plasma is present, collective acceleration of positive ions occur, and the resulting charge neutralization enables the beam to propagate. Experimental results, theoretical understanding, and schemes to achieve high ion energies by external control of the beam front velocity will be reviewed.

1. INTRODUCTION

When an intense relativistic electron beam (IREB) is injected into a metal drift tube, or encounters a discontinuity in its environment, such that the beam current exceeds the space charge limiting current, it stops propagating. A "virtual cathode" associated with very high charge density and electric field gradients (10^2 to 10^3 MV/m) develops at the beam front and the electrons are decelerated and reflected by the negative space-charge potential. When the drift tube is filled with a neutral gas at a suitable pressure (e.g. H_2 at $\sim$ 0.1 Torr) or when a plasma is present at the entrance of the drift tube, collective acceleration of positive ions from the gas or plasma occurs, and the resulting charge neutralization enables the beam to propagate. This effect was first discovered accidentally by Graybill and Uglum in 1968 during experiments with an intense electron beam in a gas-filled drift tube[1]. The typical geometry of such an experiment is illustrated in Fig. 1a.

After the discovery of Graybill and Uglum, many experiments with gas-filled drift tubes were performed during the early seventies. It was found that the peak ion energy increased with pressure until an upper pressure limit is reached beyond which no ion acceleration occurs. For ions with positive charge Ze, the kinetic energy, E_i, can be expressed in terms of the electron kinetic energy, E_e, or the electron beam voltage, V_b, as

---

*presently on leave at GSI Darmstadt with support from the Alexander von Humboldt-Stiftung (Humboldt Award)

$$E_i = \alpha Z E_e = \alpha Z e V_b \quad , \qquad (1)$$

where α is the energy amplification factor. The experimental energy spectrum has an exponential shape with an effective value of $\alpha \simeq 1$ for the bulk of the ions and with $\alpha \sim 3\text{-}10$ for a distinct high-energy tail. Though many theoretical models were proposed, the best explanation of the many experimental observations was given by Olson in his comprehensive theory.[2] Olson also proposed the Ionization Front Accelerator (IFA) as a scheme to control the beam front propagation velocity and thus achieve higher ion energies. We will discuss this scheme in Section 3 of this paper.

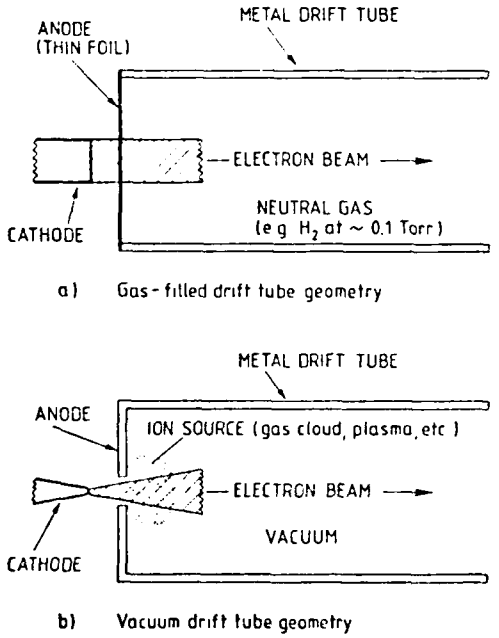

Figure 1

Typical experimental configurations for collective ion acceleration with intense relativistic electron beams (IREB): (a) IREB injection into drift tube filled with neutral gas, (b) IREB injection through localized gas cloud or plasma into a vacuum drift tube.

In 1974, J. Luce at Livermore pioneered a somewhat different collective ion acceleration method[3]. He used dielectric material in the anode of the IREB generator and injected the electron beam through a hole in the anode into a vacuum drift tube. With such a system, now known as a "Luce diode", and by using special ring-shaped electrodes (called "lenses" by Luce) in the vacuum drift tube, he reported ion energies that were significantly higher than those in the gas filled drift tubes. The highest value

for the amplification factor reported by Luce was [illegible] for [illegible]. Subsequently, experiments with "Luce diodes" were performed at the University of Maryland and several other laboratories. The Maryland group, recognizing that the dielectric served as the source of positive ions, developed a new system which provided better reproducibility and external control of the experiments. In this new configuration, the dielectric is replaced by a standard metal anode and the electron beam is injected into the vacuum drift tube through a well localized ion source in the form of a gas cloud or a laser-produced plasma. This system is shown in Fig. 1b. In experiments with such a system, positive ions of various gas and metal species were accelerated to peak energies of about 5 MeV per nucleon[4]. The total kinetic energy of about 900 MeV for Xenon ions is the highest energy achieved so far in collective acceleration experiments anywhere.

In contrast to the experiments with neutral gas, the results obtained in vacuum drift tubes are not yet fully understood. However, theoretical studies at the University of Maryland have identified several key features of the acceleration mechanism. In particular, a moving virtual cathode appears to be most consistent with the experimental data. The motion of the beam front and the virtual cathode can be influenced by the use of special electrodes (as was demonstrated by both Luce and the Maryland group). This led to the proposal of the helix-controlled Beam Front Accelerator (BFA) which is now being studied at the University of Maryland. The BFA concept will be discussed in Section 4.

Collective ion acceleration in the beam front motion schemes (IFA, BFA) is intimately connected with the propagation of electron beams near or above the space-charge limit. Therefore, in Section 2, we shall first present a brief review of the various phenomena that limit the propagation velocity of an IREB in neutral gas or vacuum. Before doing so it is worthwhile to point out some major differences between the beam front accelerators (IFA, BFA), on the one hand, and the Electron Ring Accelerator (ERA) and the Wave Accelerators, on the other hand. Both the ERA and the wave accelerators originated from theoretical ideas by Veksler, Budker and Feinberg in the fifties before intense relativistic electron beam generators were developed and experiments performed. By contrast, the beam front accelerator concepts evolved from theoretical analyses of experimental observations that occurred almost accidentally and that were neither expected nor predicted. It took many years of research and development to

achieve collective ion acceleration in the ERA; wave accelerators have not been successful so far though the generation of slow waves with modest electric field gradients (∿ 10 MV/m) has been demonstrated. However, the parameter dependence and scaling in these schemes is well understood since they are based on theoretical models. By contrast, collective ion acceleration in the beam front accelerator occurs naturally; the problem is to understand the observation and to control the natural processes and to develop scalable acceleration schemes. Another difference is the fact that beam front accelerators operate at higher currents (near and above the space charge limit), and that the field gradients in the beam front accelerators are at least one order of magnitude greater than in the ERA and wave accelerator cases.

2. LIMITING CURRENTS AND ELECTRIC FIELD GRADIENTS IN INTENSE RELATIVISTIC ELECTRON BEAMS

The electron beams used in these collective ion acceleration experiments are single pulses, typically between 10 and 100 ns long, with peak currents in the range from 10 to 100 kA, and peak energies between 0,5 to 5 MeV. All experiments so far have been done on a "single-shot" basis, i.e. one shot at a time which is repeated every few minutes. Repetition rate capability for these accelerators is being developed at Sandia Laboratories and at Livermore. A high-voltage pulse is applied to a diode (cathode-anode), and the electrons emitted from the cathode are accelerated and injected into a metal drift tube through either a thin foil or a hole in the anode. In the drift tube the electron beam can be focused by applying a uniform axial magnetic field or via charge neutralization if a neutral gas is present.

The electron beam generates very high electric and magnetic fields which have a strong effect on the motion of individual electrons. Moreover, the energy stored in these fields must be supplied from the kinetic energy of the beam. If a neutral gas is present, ionization takes place by collision with the beam electrons. The secondary electrons from these ionizing collisions are instantly ejected from the beam region to the walls and the remaining positive ions provide partial or full charge neutralization of the electron beam. Comoving or counterstreaming ions and electrons may also affect a partial or full current neutralization.

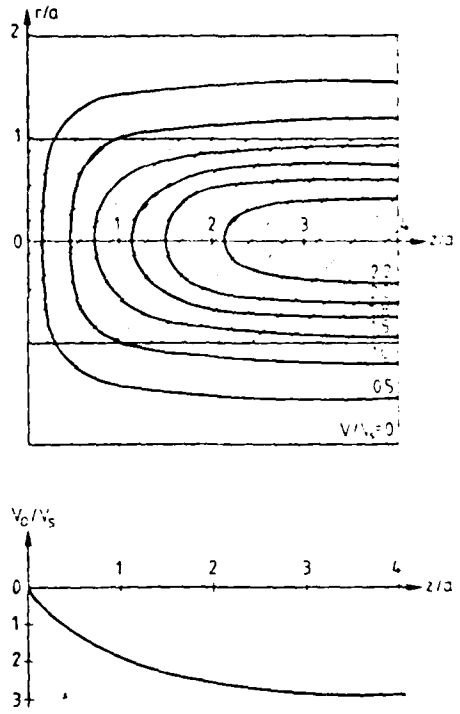

Figure 2

Potential distribution of electron beam with radius a entering a drift tube with radius b = 2a. Top: equipotential lines in units of V_s = 30 I/β. Bottom: potential variation along beam axis.

Fig. 2 shows the electrostatic potential distribution of a cylindrical beam with radius a and uniform charge density injected into an evacuated metal drift tube with radius b. The equipotential lines are shown near the anode for the case b = 2a. Potentials are indicated in units of

$$V_s = \frac{I}{4\pi\varepsilon_o v} = \frac{30\ I}{\beta} \quad . \tag{2}$$

At a distance z >2b, the electric field has only a radial component (assuming a constant beam radius in this uniform beam model). The potential difference between beam axis (r = 0) and beam edge (r = a) is V_s, given in (2). The potential difference between beam axis (r = 0) and wall (r = b) is

$$V_o = V_s\ (1 + 2\ \ln\ b/a)\ , \tag{3}$$

and the maximum radial electric field at the beam edge (r = a) is

$$E_{r,max} = \frac{2V_s}{a} = \frac{60\ I}{\beta a} \quad . \tag{4}$$

As an example, for $I = 3\times10^4$ A, $\beta = 1$, $a = 6\times10^{-3}$ m, $b = 2a$, one gets $V_s = 0.9$ MV, $E_{max} = 300$ MV/m, and $V_o = 2.15$ MV. Thus, if V_b denotes the accelerating diode voltage, the kinetic energy of the electrons, eV_b, must be greater than eV_o to overcome the negative potential barrier on the beam axis. In our example we must have $eV_b > 2.15$ MeV. Incidentally, from the calculated field pattern of Fig. 2, one infers that there is a high axial electric field at the anode plane ($z = 0$, $r = 0$) given by

$$E_{z,max} \approx \frac{75\ I}{\beta a} \ . \tag{5}$$

In our example this implies a gradient of 375 MV/m.

What happens when the potential on the beam axis approaches the accelerating diode voltage ? As $V_o \to V_b$, the beam is stopped by its own space charge, and the electrons are reflected back to the anode. The current where this limit occurs is known as the space-charge limiting current. It was first derived by Bogdankevich and Rhukadze in 1971 and may be expressed in the form[5)]

$$I_L = I_o \frac{(\gamma_b^{2/3} - 1)^{3/2}}{(1 + 2 \ln b/a)\ (1 - f_e)} \ , \tag{6}$$

where $I_o = \frac{4\pi\varepsilon_o\, mc^3}{e} \approx 1.7\times10^4$ A for electrons, and γ_b is the relativistic energy factor defined as

$$(\gamma_b - 1)\ mc^2 = eV_b \ . \tag{7}$$

The factor f_e in the denominator represents fractional space charge neutralization by positive ions.

In addition to the radial electric field E_r, there is an azimuthal magnetic field B_θ due to the beam current. The associated Lorentz force $v_z B_\theta$ on the beam electrons is radially inward, i.e. focusing and counteracting the repulsive electric force. A net strong focusing force results when the space charge field is neutralized ($f_e = 1$). As was first shown by Alfvén[6)] and later by Lawson[7)], this force stops and reflects the beam electrons (pinch effect) when the current exceeds the critical limit

$$I_A = I_o \beta\gamma = 1.7 \times 10^4 (\gamma^2-1)^{1/2} \text{ A} . \qquad (8)$$

Note that $I_A > I_L$.

The energy stored in the electric and magnetic self fields of an electron beam of length L is given by

$$W = \frac{I^2 L}{4\pi\varepsilon_o c^2} \left(\frac{1}{4} + \ln \frac{b}{a}\right) \left[\frac{(1-f_e)^2}{\beta_f^2} + (1 - f_m)^2\right] , \qquad (9)$$

where f_e represents the fractional charge neutralization and f_m the fractional current neutralization.

This field energy must be supplied from the kinetic energy of the beam electrons, i.e. the kinetic energy at the beam front equals the kinetic energy at injection minus the field energy. This energy conservation law may be expressed in the form of a power balance, namely

$$I(\gamma_f - 1) \frac{mc^2}{e} = I(\gamma_o - 1) \frac{mc^2}{e} - \frac{W}{L} \beta_f c . \qquad (10)$$

Of particular interest is the case of a charge-neutralized beam ($f_e = 1$) where an upper limit is reached when $v_f = 0$, i.e. all of the injected beam power is converted into magnetic field energy. The current in this power-balance limit is given from Eqs. (9) and (10) by

$$I_p = I_A \frac{4}{1 + 4 \ln b/a} \frac{\gamma_b(\gamma_b - 1)}{\gamma_b^2 - 1} . \qquad (11)$$

It differs from the magnetic limit I_A mainly by the geometry factor $4/(1 + 4 \ln b/a)$ which represents the field between beam (r = a) and wall (r = b) that was neglected by Alfvén and Lawson. Solving (10) for β_f in the case $\gamma_f = 1$ ($v_f = 0$), one obtains an upper limit, the so-called power-balance limit, for the beam front velocity:

$$\beta_f = \frac{V_b}{I} \frac{1}{7.5 (1 + 4 \ln b/a)} . \qquad (12)$$

This limit plays an important role in the Olson theory of collective ion acceleration in neutral gas[2], as will be discussed in the next section.

The above theory, in particular the space-charge limiting current, was based on the nonphysical "uniform" beam model which by implication assumes that an infinite axial magnetic field forces all electrons to travel along straight lines. A more accurate self-consistent theory of a magnetically focused electron beam was presented by the author in 1977[8]. It yields the following relations for the beam current I, the relativistic energy factor γ_b, and the applied uniform magnetic field B_o:

$$I = \frac{I_o}{2} (\gamma_o^2 - 1)^{1/2} \left(\frac{\gamma_a^2}{\gamma_o^2} - 1\right) \quad , \tag{13}$$

$$\frac{\gamma_b}{\gamma_o} = \frac{\gamma_a}{\gamma_o} + \left(\frac{\gamma_a^2}{\gamma_o^2} - 1\right) \ln \frac{b}{a} \quad , \tag{14}$$

$$B_o = \frac{mc}{ea} \left(\frac{\gamma_a^2}{\gamma_o^2} - 1\right)^{1/2} \left[\left(\frac{\gamma_a}{\gamma_o} + 1\right) - \left(\frac{\gamma_a}{\gamma_o} - 1\right) \frac{a^2}{b^2}\right] \quad , \tag{15}$$

where γ_o, γ_a, γ_b refer to the electron energy at the beam axis (r = 0), beam edge (r = a) and wall (r = b).

These three equations relate the experimental parameters I, γ_b, B_o, a, b; given two of the five parameters one can calculate the other three quantities.

From the above equations we can derive the modified space-charge limiting current by setting $\partial I/\partial \gamma_o = 0$. In the case b = a, one finds for γ_o the relation

$$\gamma_o^2 = \frac{\gamma_a^2}{2} \cdot \left[(1 + 8\, \gamma_a^{-2})^{1/2} - 1\right] . \tag{16}$$

Substitution of (16) into (13) yields the space-charge limiting current. Finally, we note that the beam front velocity in this self-consistent model is defined as

$$\beta_f = \frac{(\gamma_o^2 - 1)^{1/2}}{\gamma_o} \quad . \tag{17}$$

Let us now briefly discuss what happens when the beam current exceeds the space-charge limiting current I_L. Only a simplified, one-dimensional theory yields analytical answers in this case. For $I > I_L$, one finds that

a virtual cathode forms at a very small distance d_m from the anode (injection) plane. The charge density at the virtual cathode is many times greater than the injected beam density, and the potential at the minimum, V_m, may be less than the cathode potential V_b, as illustrated in Fig. 3. Both d_m and V_m oscillate with small amplitudes about mean values obtained from the theory.

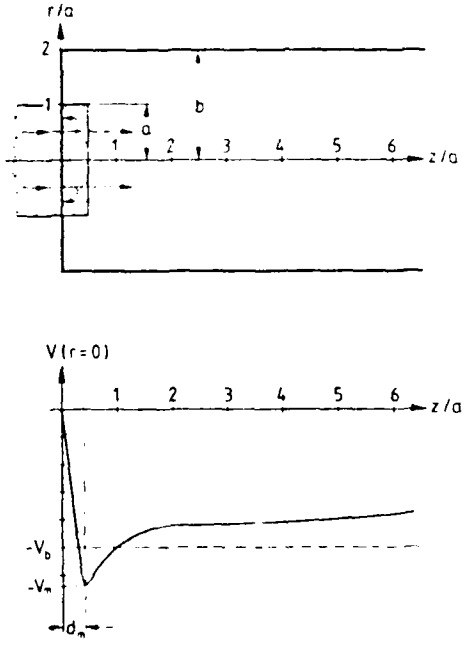

Figure 3

IREB injection into drift tube when current is above the space-charge limit ($I > I_L$). Top: Beam front stops at short distance d_m from anode, electrons are reflected. Bottom: Typical potential variation along beam axis; the potential minimum V_m at virtual cathode exceeds the beam voltage V_b.

Of particular importance with regard to collective ion acceleration is the electric field at z = 0 which may be expressed in the form

$$E[MV/m] = \frac{2.04}{a_{[m]}} \left(\frac{I}{I_o}\right)^{1/2} (\gamma_b^2 - 1)^{1/4} . \qquad (18)$$

As an example, for $I = 2I_o = 34$ kA, $\gamma_b = 3$, $a = 10^{-2}$ m, one finds $E = 485$ MV/m. On the other hand, for $I = 5I_o = 85$ kA, $\gamma_b = 5$ and $a = 10^{-2}$ m, one obtains $E = 1{,}010$ MV/m. These high electric field gradients and the potential well associated with the virtual cathode at the beam front play, according to our understanding, a crucial role in the observed collective ion acceleration processes, as will be discussed in the next two sections.

3. COLLECTIVE ION ACCELERATION IN NEUTRAL GAS, THE ITA CONCEPT

When an IREB is injected into a metal drift tube filled with neutral gas at a pressure p, ionization of the gas molecules by the electrons takes place. As positive ions are formed and accelerated in the electrostatic potential well of the beam, they too can contribute to ionization by collision with gas molecules. Following Olson's theory[2], the most important parameter determining the physical effects is the time τ_N it takes to neutralize the space charge of the beam (i.e. the ion density equals the electron density). For hydrogen gas (H_2) Olson obtained the relation

$$\tau_N \sim 1.0\ [p(\text{Torr})]^{-1}\ \text{nsec}\ , \tag{19}$$

i.e. τ_N is inversely proportional to the pressure p, as one expects. The beam physics and ion acceleration depend on the rise time t_R and total pulse length t_p of the electron beam and the pressure p of the neutral gas.

In the low pressure regime ($p < p_T$, $\tau_N > t_p$), a virtual cathode forms, the electrons are reflected and no beam propagation occurs. It is assumed, of course, that the beam current during the entire pulse length remains above the space-charge limit. Positive ions created in the potential well of the electron beam can be accelerated to kinetic energies of $E_i \leq eV_b$ (assuming a potential well depth of $V_o \cong V_b$).

In the high pressure regime ($p > p_T$, $\tau_N < t_p$), the beam becomes fully neutralized in time τ_N which is less than the pulse duration t_p. The beam, therefore, is able to propagate with a beam front velocity $\beta_f = L_W/\tau_N c$, where L_W is the width of the well region. Positive ions trapped in the moving potential well on the beam front are accelerated to a maximum velocity of $v_i \cong v_f \cong L_W/\tau_N$, which in view of (19) increases with gas pressure p. When the gas pressure gets high enough such that the electron beam gets neutralized during its rise time t_R before the current I reaches the limiting value I_L, no virtual cathode forms, the beam never stops and no ion acceleration should occur. The condition for this to happen is $\tau_N \leq \tau_R = (I_L/I)t_R$. Olson calls it the "runaway regime". Fig. 4 illustrates the beam front and ion velocity variation with pressure for the three regimes. At pressures $p > p_R$, where no ion acceleration takes place, the electron beam front velocity is limited by the power-balance relation (12). In most experiments this velocity was significantly greater than the

maximum ion velocity observed, in agreement with Olson's theory.

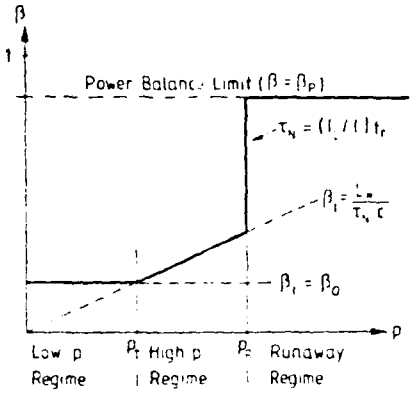

Figure 4

Electron beam front and ion velocity variation with neutral gas according to Olson's theory.

It is clear from the above model that further increase of the ion energies can be achieved only by avoiding the runaway effect, i.e. by external control of the beam front velocity. Olson proposed to accomplish such control in the Ionization Front Accelerator (IFA) concept schematically shown in Fig. 5. The drift tube is filled with a "working gas" at a pressure low enough that ionization by beam electrons is insignificant. Instead, the intense light pulse from a laser source is used to ionize the gas. Light pipes of increasing length allow one to control the arrival time along the drift tube and thus the propagation velocity of the beam front. Positive ions trapped in the unneutralized space charge well at the head of the beam are accelerated as the well propagates with increasing velocity that is determined by the arrival sequence of the laser pulses. The upper limit for the beam front and ion velocity is given by the power balance relation (12). Olson estimated that a 100 ns IREB pulse should be more than sufficient to achieve 1 GeV protons.

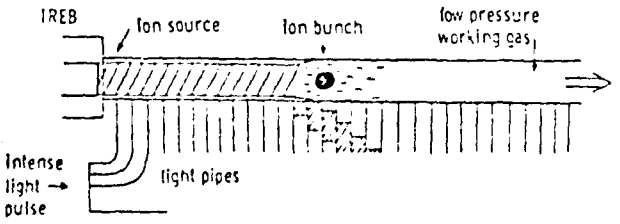

Figure 5

The Ionization Front Accelerator (IFA) scheme. The IREB is charge-neutralized by laser-light ionization of a low-pressure working gas. The unneutralized beam front forms a potential well for positive ions. Beam front velocity and thus ion acceleration is controlled by arrival of light pulses via light pipes of increasing length. (Courtesy of C.L. Olson).

It is important to point out that the IFA scheme can also operate below the space charge limit I_L. In this case the electron beam propagates even without the laser. However, the laser ionization produces a sharp transition within the beam pulse behind which the beam is fully neutralized and in front of which the space charge is unneutralized. Again one obtains an ionization beam front which travels at an increasing velocity (less than the actual beam front) as determined by the sweep of the laser pulses.

After completion of a "proof-of-principle" experiment (IFA-1) with encouraging results (proton energies of about 5 MeV), Olson has recently started the "test bed accelerator" project (IFA-2). This project aims at proton energies of 100 MeV. It features an improved electron beam generator with better reproducibility and low jitter, and a new working gas (NN dimethyl aniline - DMA) that operates at room temperature and requires only one laser (XeCl) for the ionization process[9]. Results with this new system are expected within the next year.

4. COLLECTIVE ION ACCELERATION IN VACUUM, THE BFA CONCEPT

The physical mechanisms involved in collective ion acceleration when an IREB is injected through a gas or a plasma (see Fig. 1b) into a vacuum drift tube are not as fully understood yet as in the neutral gas case. However, the experimental data at the University of Maryland are consistent with a moving virtual cathode. Positive ions produced by collisions in the gas cloud or by laser bombardment of a solid target material are accelerated by the strong electric field of the virtual cathode that forms on the vacuum side of the gas cloud or plasma. The positive ions neutralize the electron space charge and, as a result, the electron beam front with the virtual cathode moves further down-stream. This "self-synchronized" propagation of electrons and co-moving ions depends on the ion density in the gas cloud or plasma, the rise time and pulse length of the electron beam, the drift tube geometry, the ratio of beam current to the space-charge limiting current, the beam voltage, and other factors. Many more systematic experiments will be required to explore the parametric dependence and to optimize the ion acceleration process. The major results of our studies at the University of Maryland so far can be summarized as follows:

a) The maximum proton energy increases roughly with the square root of the electron beam power, i.e. $E_i \propto (IV_b)^{1/2}$. This is in reasonable agreement with the formula (18) for the maximum electric field of the virtual cathode.

b) Positive ions of various gas species (from H to Xe) were accelerated to the same peak velocity of $v = 0.1\ c$ (corresponding to a kinetic energy of 5 MeV/n) independent of the ion mass. This result supports the concept of a moving potential well. We have so far, however, no satisfactory explanation why the peak velocity was 0.1 c in our experiments. Further systematic investigations showing how this velocity depends on experimental parameters have to be carried out in the future.

c) The total charge of the accelerated ion bunches is roughly constant (independent of ion species). This result indicates that the electron beam propagates as soon as a certain amount of fractional charge neutralization, f_e, is reached. It also shows indirectly that the number of accelerated ions is inversely proportional to the mean charge state of the ion distribution.

A special advantage of the evacuated drift tube compared with the neutral gas case is the fact that one can place electrodes into the beam path and try to control the beam front velocity. Preliminary experiments with one or two ring-shaped electrodes[10] and subsequently with helical structures were very successful. Such "slow-wave" structures affect the beam front motion and allow a group of accelerated ions to remain in step with the potential well at the head of the electron beam. So far, we have demonstrated that a group of ions at the high-energy tail can be separated from the low-energy distribution and accelerated to higher energies[10]. A factor 2 increase of the ion energy was achieved so far.

The early success with one or two ring-shaped electrodes led to the development of the helix-controlled beam front accelerator[11] which is schematically illustrated in Fig. 6. After passage through the gas cloud or plasma and initial ion acceleration, the electron beam enters a slow-wave helical structure. The inner radius b of this structure is chosen small enough that the space-charge limiting current is greater than the beam current when the helix is at ground potential. However, if the helix is charged to a sufficiently high negative potential, the limiting current

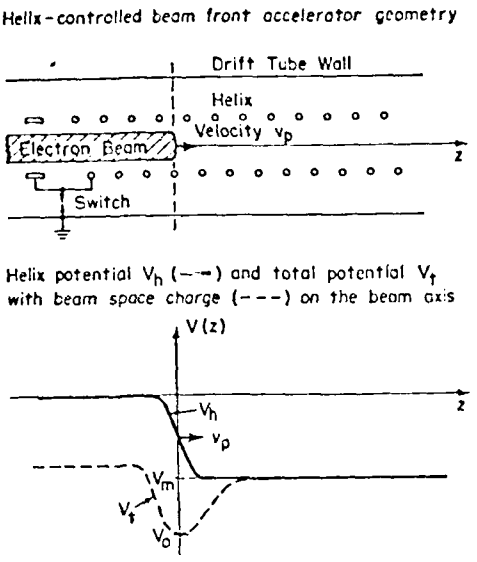

Figure 6

The Beam Front Accelerator (BFA) scheme: A slow-wave structure (e.g. helix) inside the vacuum drift tube is charged to negative potential V_h which is grounded with a switch when the IREB arrives. The grounding wave traveling along the structure with phase velocity v_p controls the beam front velocity and thus the acceleration of positive ions in the potential well at the beam front. (a) Schematic of experimental configuration. (b) Electrostatic potential variation along beam axis at time corresponding to beam front location shown in (a); positive ions trapped in potential well at beam front are accelerated as $v_p(t)$ increases with distance z.

decreases below the beam current and beam propagation stops. The energy factor γ_b in Eq. (6) must be replaced by $\gamma_b - \gamma_h$, where $(\gamma_h - 1)\, mc^2 = eV_h$ represents the decrease of the electron kinetic energy due to the negative helix potential V_h. The helix can be discharged by triggering a switch at the upstream end. The discharge voltage pulse, which grounds the helix, travels downstream with a phase velocity v_p that depends on the pitch angle angle Ψ of the helical structure and is given by

$$v_p \cong c \sin \Psi \tag{19}$$

for high frequencies. By increasing the pitch angle one can increase the beam front velocity and thereby the energy of the ions that are trapped in the potential well of the virtual cathode.

In our experiments so far, the helix was charged up by the initial part of the electron beam pulse. The gap in the switch was adjusted such that voltage breakdown occurs when a threshold value is exceeded. Helix charging by an external geenerator and external triggering of the switch have to be studied in the future. It may in fact not be necessary since the image charges and currents in a slow-wave structure travel with velocity v_p which may be sufficient to slow down the beam front[12].

5. ELECTRON BEAM PROPAGATION AND COLLECTIVE ION ACCELERATION, THE "PISTON-PLASMOID" MODEL

From the previous discussion it is clear that electron beam propagation and collective ion acceleration are intimately connected. In a metal drift tube, an intense electron beam can propagate only when the beam current I is less than the space charge limit I_L. If not, propagation requires the presence of a charge-neutralizing positive ion background so that $I < I_L$.

When the drift tube radius is very large or when the electron beam is injected into free space (ideal vacuum), the space charge limiting current is practically zero ($I_L \approx 0$). Electron beam propagation in this case is possible only when co-moving positive ions are present. (An analogous situation exists in ion propulsion where co-moving electron beams are generated to neutralize the positive ion beam that emerges from the rocket engine.) When an intense electron beam is injected into free space from a solid conducting surface, the virtual cathode due to the negative space charge becomes a "mirror" which reflects all electrons back to the surface. If the solid conductor is replaced by a plasma with mobile charged particles, positive ions are extracted from the plasma surface and accelerated by the electric field associated with the electron space charge mirror. Provided that the plasma and ion density is sufficiently high, the layer of accelerated ions fully neutralizes the electron beam and the reflecting space charge mirror moves further downstream. The electron mirror in front of the electron and co-moving ion beam can be compared with the action of a "piston"[13]. This action which forces positive ions to follow the electrons is,in a sense,self-synchronizing and should continue, in principle, until the electron pulse terminates, or the supply of ions is cut off, or the co-moving ions have reached the same velocity as the injected electrons, whichever comes first. In the last case, the mirror disappears, no further electron reflections occur, electrons and co-moving ions form a charge and current-neutralized "plasmoid". Since the electric and magnetic fields associated with such a "plasmoid" are practically zero, no kinetic energy of the electron beam is converted into field energy. This "piston-plasmoid" model thus provides a mechanism by which ions are accelerated to the velocity of the injected electrons. The process is illustrated in Fig. 7 which shows schematically the various phases of the advancing electron and ion charge density

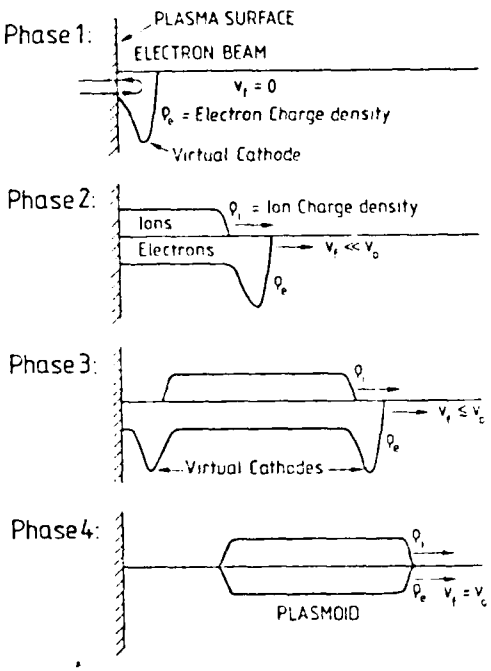

Figure 7

Suggested phases of plasmoid formation when an intense electron beam is injected into free space through a high-density plasma. Phase 1: Electron charge density ρ_e with virtual cathode (mirror) at time of injection. Phase 2: Positive ions of charge density ρ_i are extracted from plasma; beam front with virtual cathode moves with velocity $v_f \ll v_o$ (= electron velocity at injection). Phase 3: As v_f approaches v_o, a second virtual cathode (mirror) forms upstream separating the electron-ion bunch. Phase 4: The charge- and current-neutralized plasmoid ($\rho_i = \rho_e$, $v_i = v_o$) propagating with velocity $v_f = v_o$.

distributions. Just before the plasmoid state is reached, a second virtual cathode or electron mirror forms upstream from the beam front. This mirror prevents the reflected electrons from leaving the plasmoid and thereby separates the plasmoid from the rest of the beam.

In this model, the virtual cathode or mirror at the front of the advancing electron beam provides a mechanism to transfer energy to the positive ions. Indeed, each reflected electron gives up momentum in the amount

$$\Delta p = 2p_e = 2mc\beta_e\gamma_e \ , \qquad (20)$$

which is transferred to the positive ions extracted from the plasma. Let $J_e = en_e v_e$ denote the electron flux, v_i and M the velocity and mass of the ions, n_i the ion density, and L the length of the ion bunch. The momentum transfer (per second and square meter) from the reflecting electron stream to the ion bunch is then[13)]

$$\frac{dp}{dt} = \frac{d(Ln_i M v_i)}{dt} = 2\, n_e \gamma_e m (v_e - v_i)^2 \quad . \tag{21}$$

For Ln_i = const, one obtains in the non-relativistic approximation the result

$$v_i = v_e \left\{ 1 - \left[1 + \frac{2 n_e \gamma_e m}{M L n_i} \; v_e \; (t - t_o) \right]^{-1} \right\} \quad . \tag{22}$$

which indicates that $v_i = v_e$ for $t \to \infty$.

This rather simple analytical model needs to be refined and studied by numerical simulation. However, the main question is whether such plasmoids can be formed in laboratory experiments. There are a few observations which seem to indicate that short ion pulses with a current comparable to that of the electron beam have been generated. But further studies are needed to obtain conclusive data to test the validity of the piston-plasmoid model. The fast ion tail ejected together with electrons from the plasma formed by bombardment of small pellets or other solid targets with a high-power laser beam also suggest that such a plasmoid effect takes place. It may well be that this mechanism plays a role in cosmic ray acceleration. As is known from laser fusion and other studies, a large amount of the available energy generates streams of relativistic electrons. An energy-releasing event on the surface of a star could produce intense jets of high-energy electrons. These electrons cannot escape into the vacuum of free space. They are reflected by their own space charge which in turn provides a mechanism to accelerate ions from the plasma on the surface of the star.

To summarize, the key feature of the plasmoid model is that many reflecting electrons transfer momentum and thus kinetic energy to a small group of ions until the ions have been accelerated to the same velocity as the injected electrons. The question remains to be answered whether laboratory conditions can be achieved in which such self-synchronized ion acceleration and plasmoid formation takes place or whether we must rely on external control as in the IFA or BFA concepts discussed in the previous sections.

6. CONCLUDING REMARKS

It is interesting to compare the flow of energy in a conventional high-energy accelerator with that in a collective accelerator. In the conventional system, the electric energy from the power source is first converted into kinetic energy of the electron beams in the micro-wave tubes (Klystrons, etc.). This kinetic energy of electrons is then converted into the radio-frequency waves that finally accelerate the charged particles. Depending on the power requirements many such r.f. generators or amplifiers are placed at suitable intervals along the particle accelerator.

The collective acceleration with intense relativistic electron beams discussed here by-passes the r.f. generation and converts electron kinetic energy directly into positive ion energy. Whether this can be done in a controlled fashion and used to achieve ultra-high energies remains an open question and a great challenge for accelerator physics. Single-staged IFA or BFA devices, as described in this paper, will undoubtedly be limited to energies considerably below the TeV range required from an ultra-high energy accelerator. As with conventional r.f. power amplifiers, staging of collective accelerators would be necessary. The amount of kinetic energy that can be transferred to ions in each stage depends on the power IV_b and pulse length t_p of the electron beam. The upper limit for the achievable ion energy is given by the relativistic energy factor γ_e of the last electron beam generator. This applies both for beam front accelerators as well as for wave accelerators. If we take the design energy of 50 MeV of the ATA project at Livermore as a realistic, near-term goal, than $\gamma_e = \gamma_i = 100$, corresponding to a proton energy of about 100 GeV. To go beyond this limit, one has to explore "fast" waves - either shocks or harmonic waves - that travel along the electron beam pulse from the rear to the front with a speed greater than the electron velocity. At present the main objective of the existing collective accelerator projects is to demonstrate the feasibility of "slow-wave" schemes designed to accelerate ions from rest to energies in the range between 10 and 1000 MeV. The problems of staging and "fast-wave" schemes (which require the injection of relativistic ions) can be explored after these experiments have been successful.

REFERENCES

1) S.E. Graybill and J.R. Uglum, J. Appl. Phys. 41, 236 (1970); S.E. Graybill, IEEE Trans. NS-19, 292 (1972).

2) C.L. Olson and U. Schumacher, Springer Tracts in Modern Physics: Collective Ion Acceleration, (Springer, New York, 1979), Vol. 84.

3) J.S. Luce, An. N.Y. Acad. of Sci., Vol. 251, 217 (1974).

4) W.W. Destler, L.E. Floyd, and M. Reiser, Phys. Rev. Lett. 44, 70 (1980); L.E. Floyd, W.W. Destler, M. Reiser, and H.M. Shin, J. Appl. Phys. 52, 693 (1981).

5) L.S. Bogdankevich and A.A. Rhukadze, Usp. Fiz. Nauk. 103, 609 (1971) [Sov. Phys. - Usp. 14, 163 (1971)].

6) H. Alfvén, Phys. Rev. 55, 425 (1939).

7) J.D. Lawson, J. Electr. Contr. 3, 587 (1957); J. Electr. Contr. 5, 146 (1958).

8) M. Reiser, Phys. Fluids, 20, 477 (1977).

9) C.L. Olson, J.R. Woodworth, C.A. Frost, and R.A. Gerber, IEEE Trans. NS-28, 3349 (1981).

10) C.N. Boyer, H. Kim, and G.T. Zorn, Proc. Int. Top. Conf. E-Beam Res. and Tech., Albuquerque, New Mexico, Nov. 3-5, 1975 (National Technical Information Service, Springfield, Virginia, 1976), Vol. 2, p. 347.

11) W.W. Destler, H. Kim, G.T. Zorn, and R.F. Hoeberling, in Collective Methods of Acceleration, edited by N. Rostoker and M. Reiser (Harwood Academic Publishers, New York, 1979), p. 509.

12) W.W. Destler, private communication.

13) W.W. Destler, H.S. Uhm, H. Kim, and M. Reiser, J. Appl. Phys. 50, 3015 (1979).

COMPACT PULSED ACCELERATOR*

M. J. Rhee and R. F. Schneider

Laboratory for Plasma and Fusion Energy Studies
University of Maryland
College Park, Maryland, 20742

Summary

The formation of fast pulses from a current charged transmission line and opening switch is described. By employing a plasma focus as an opening switch and diode in the prototype device, a proton beam of peak energy 250 keV is produced. The time integrated energy spectrum of the beam is constructed from a Thomson spectrograph. Applications of this device as an inexpensive and portable charged particle accelerator are discussed.

Introduction

To date, the pulse forming lines (PFL) evolved from lumped capacitor circuit systems have been used to produce short, fast rising, high power pulses. Since the energy in these systems is stored in the electric field in the dielectric of the transmission line, the maximum stored energy density is limited by the dielectric breakdown strength. For the most commonly used dielectrics, water and transformer oil, the breakdown field strength is empirically found[1] as $E_{br}\, t^{1/3}\, A^{1/10} = k$. Typical breakdown strength for a practical system which has an electrode area A = 1000 cm^2, microsecond charging time, and k = 0.5 is about 25 MV/m, thus the corresponding maximum energy densities are about 200 kJ/m^3 for water and 7 kJ/m^3 for transformer oil.

Recently we reported[2] that magnetic field energy can be stored in the transmission line and a rectangular high power pulse can be produced into a matched load. In contrast to electric field energy, the magnetic field energy density is not limited by the dielectric medium. Thus, a very high density device i.e., compact system can be built. The dielectric in this case has to hold off only the output pulse field which is half of the charging field of a conventional PFL and easily an order of magnitude shorter than the pulse charging period. The empirical breakdown field strength formula has been found to be an underestimate for such a fast pulse.[3] Therefore, the energy density of such a device can be increased easily by an order of magnitude over that of a conventional PFL. Furthermore, the bulky and expensive voltage step up device, such as a Marx generator or pulse transformer, employed in most pulsed power systems can be eliminated.

In this paper, we will describe our analysis of pulse formation from a current charged transmission line, a prototype experimental device, and preliminary results of ion beam production and its energy spectrum analysis.

Current Charged Line and Pulse Formation

Analogous to the pulse formation from the (voltage) charged transmission line, one can show that a rectangular pulse can be formed from a current charged transmission line and an opening switch system, by using basic transmission line theory. A simple transmission line of length ℓ and of characteristic impedance $Z_o = (L/C)^{1/2}$, is initially shorted at both ends, and is charged with a constant current I_o as shown in Fig. 1. The current charging can be considered as a superposition of two traveling waves of constant voltage amplitudes $V^+ = -V^- = Z_oI_o/2$ and accompanying currents $I^+ = I^- = I_o/2$, proceeding in opposite directions, each being constantly reflected from the shorted ends satisfying the boundary conditions i.e., reflection coeficient $\rho = -1$. The resultant voltage along the line is zero, while the current is equal to the charging current I_o. When one end is suddenly opened by an opening switch, which is connected in parallel with a transmission line and/or a resistive load of matching impedance, the positively traveling wave no longer reflects and proceeds towards the load forming a rectangular pulse. The resultant output pulse has voltage $V_{out} = Z_oI_o/2$, current $I_{out} = I_o/2$, and pulse length $\tau_{out} = 2\ell\sqrt{\varepsilon}/c$.

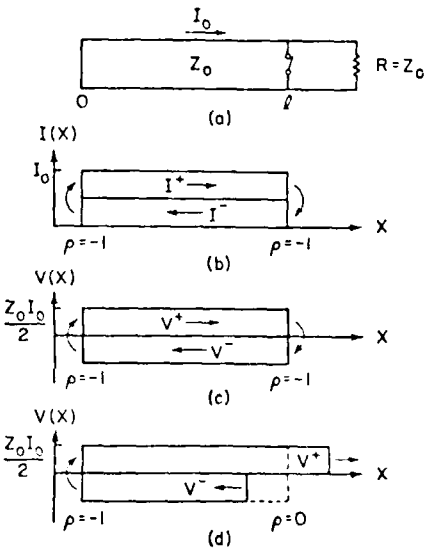

FIG. 1(a). Transmission line initially shorted at both ends and current charged with I_o, (b) Superposition of two waves I^+ and I^-, (c) V^+ and V^-. (d) When the switch opens, $V^+ = Z_oI_o/2$ and $I^+ = I_o/2$ proceeds towards the matched load.

Experiments

A prototype experimental device consists of a capacitor, spark gap switch, coaxial transmission line, and Mather geometry coaxial gun[4] which are connected in series as shown in Fig. 2. The energy initially stored in a 20 kV, 3 kJ capacitor is, by closing the spark gap, transferred to the coaxial line in the form of the magnetic field energy. The coaxial transmission line of radii a = 2.54 cm, b = 7.3 cm and length ℓ = 30 cm has total inductance of L = 64 nH. Here, we utilize the plasma focus as an opening switch and also as a plasma diode as the m = 0 instability occurs and pinches off the current carrying plasma column. The coaxial gun electrodes are made of 10 cm long copper tubing of 2.54 cm and 7.7 cm diameter respectively, and are insulated by a 2 cm long pyrex glass tube of 2.54 cm outer diameter with one end flared. Inserted between the transmission line and coaxial gun is a 2.5 cm thick diagnostics ring, in which a Rogowski coil, a $\dot{B}$ probe and a $\dot{D}$ probe are mounted. The Rogowski coil is constructed by winding 30 turns of 3 mm wide copper tape on a plexiglass ring core of 3 mm x 3 mm cross section and mean radius of

*Work supported by the Air Force Office of Scientific Research and the U.S. Department of Energy

0018-9499/83/0800-3192$01.00 ©1983 IEEE

7.65 cm and is mounted inside of the diagnostic ring. The $\dot{D}$ probe is a capacitive probe consisting of 1 cm radius disk separated 1 cm from the inner surface of the diagnostic ring. The slowest time constant for this probe is 1 ns with a water dielectric. The Thomson spectrometer is placed 60 cm downstream from the gun, and is separated by a miniature gate valve which maintains good vacuum for the spectrometer.

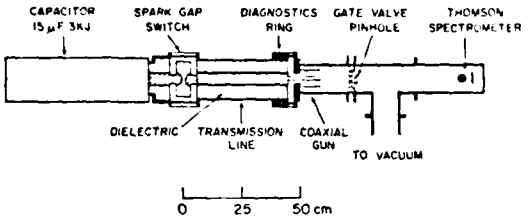

FIG. 2. Experimental setup: Prototype device and diagnostics.

The characteristic impedance of the coaxial line can be varied from 7 to 60 Ohms by using different dielectrics in the coaxial line. The output pulse characteristics strongly depend on the impedance of the transmission line as discussed in the previous section. The maximum current that can be charged through the coaxial line, is found to be 240 kA, assuming an ideal L-C circuit with charging voltage 20 kV on a 15 μF capacitor, 64 nH line inductance and 40 nH internal inductance of the capacitor. We tabulate the output characteristics of the device for reference purposes in Table I, assuming ideal circuit components such as spark gap switch, dielectrics, insulator, plasma focus as an opening switch, and a matched load.

TABLE I. Output pulse characteristics vs. dielectrics.

Dielectrics	Gases	Transformer Oil	Glycol	Water
Dielectric Constant	1	2.2	37	78.5
Characteristic Impedance (Ohm)	60	40	10	7
Output Voltage (MV)	7.2	4.8	1.2	0.84
Output Current (kA)	120	120	120	120
Pulse Length (ns)	2	3	12	18

The system is operated at a typical charging voltage of 18 kV and a fill pressure of 3 Torr hydrogen. The spark gap is triggered by activating a solenoid which opens the gate valve and then closes the trigger contact point allowing the ions accelerated to pass through, while the static filled gas pressure remains almost unchanged and good vacuum is maintained on the other side. The total current through the transmission line and the voltage induced are routinely monitored by the Rogowski coil and the $\dot{D}$ probe. Both signals are integrated by passive R-C integrating circuits with time constants of 50 μs and 2.6 μs respectively. Ions accelerated by the induced pulse voltage pass through the pinhole and the gate valve, drift further downstream, and are deflected by both the electric field and magnetic field of the Thomson spectrometer and recorded on the detector plate.

Thomson Spectrometer

A Thomson spectrometer used in this work as shown in Fig. 3 is similar in design as reported earlier.[5,6] Two round bar ceramic magnets of 2.22 cm diameter and 2.54 cm long are held together by a 10 cm diameter plexiglass disk maintaining a pole gap of 3 mm. The magnetic field in the gap is measured to be 3.5 kG. The magnets are separately connected to an external HV power supply to produce an electric field parallel to the magnetic field in the gap.

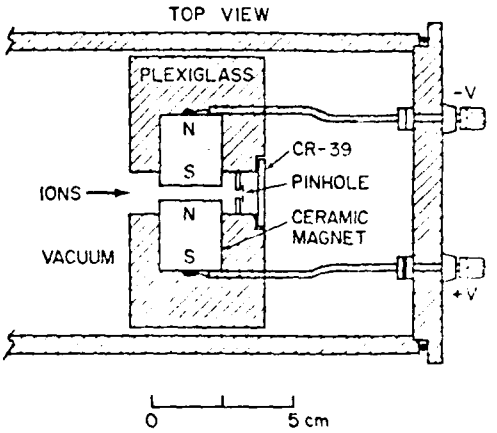

FIG. 3. Cross sectional view of Thomson spectrometer.

Immediately downstream of this field region, a 10 μm diameter pinhole on 10 μm thick nickel disk is placed. The CR-39 detector plate is placed 5 mm downstream of the pinhole. Another pinhole of variable size is placed upstream of the gate valve which is 50 cm upstream of the spectrometer, and serves as an approximate point source of ions with an intensity that depends on the pinhole size. The deflection angles of ions by the electric and magnetic fields of the spectrometer are given by

$$\theta_e = \frac{ZeEL}{2T}, \quad \theta_b = \frac{ZeBL}{\sqrt{2AMT}},$$

and can be used to measure the energy per charge and the momentum per charge respectively, where E and B are electric and magnetic field extended in length L, Z is the charge state, A is the mass number, T is the kinetic energy of the ion, and M is the unit nucleon mass based on C^{12}. The combination of both deflections gives a parabola equation which can be used to determine the charge to mass ratio of ions.

$$\theta_e = \frac{AMEL}{Ze(BL)^2}\,\theta_b^2.$$

Two shots are needed to complete a Thomson spectrograph: one shot without applied voltage to the electrodes (magnets) deflects all ions vertically, which provides a reference axis (B-axis), and a second shot with electric field by applying a voltage (1 to 10 kV) in addition to the magnetic field which makes a parabola pattern of ion tracks on the CR-39 detector plate. Since the permanent magnets are built into the system, it is difficult to make an E-axis in the horizontal direction, as done in previous works.[5,6] We have found, however, that just enough neutral ions (which may be neutralized by charge exchange or recombination process after the acceleration) are present to mark the origin of the parabola coordinates. This feature not only removes the necessity of the extra shot for the E-axis, but also allows use of small magnets built into the system, thus making operation of the system very simple. After exposure to the ion beams, the CR-39 plate is

etched in 6.25 N NaOH solution at 70°C. The etching time varies depending on the ion species, energies, and the means of reading the tracks. For protons, two hours' etching time is quite adequate for simple optical microscope reading.

Experimental Results

The voltage monitored by the $\dot{B}$ probe at diagnostic ring may be a close representation of the output voltage across the plasma diode, in which both ions and electrons are accelerated. The pulse width is measured to be ~ 20 ns which is consistent with the round trip electrical length of the water filled transmission line.

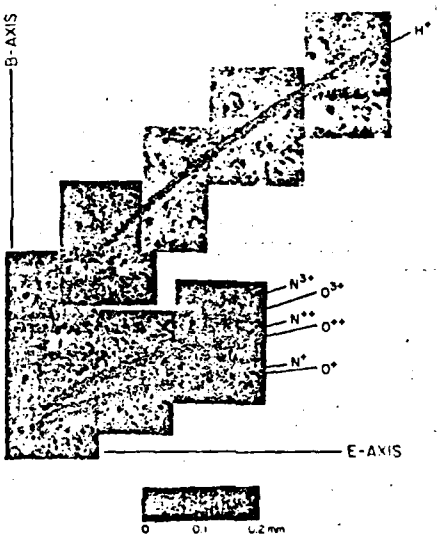

FIG. 4. Optical microscope photograph of a typical Thomson parabola showing protons and impurity ions.

The Thomson spectrometer is particularly well suited for ion beam analysis. A typical Thomson parabola taken with hydrogen filling gas is shown in Fig. 4. The size of the upstream pinhole near the gate valve is adjusted to 0.6 mm diameter which makes the density of ion tracks on the detector plate low enough to be counted by using a simple optical microscope. Each track (dot) corresponding to each ion is well separated as seen in Fig. 4. The uppermost parabola is identified as that of protons by comparing with the calculated parabola and also by track size. A few more parabolas are found below the H^+ parabola. Three distinctive ones correspond to N^+, N^{++}, and N^{+++}. The relatively low number density tracks under nitrogen parabolas correspond to O^+, O^{++}, and O^{+++}. This is attributed to the residual and/or leaked air into the vacuum chamber.

The highest and lowest energies of proton by the electric deflection are found to be 265 keV and 67 keV respectively. The lower limit is due to the narrow pole gap which limits the acceptance angle. A time integrated energy spectrum has been constructed from the H^+ parabola. The parabola is divided into many segments of constant electric deflection angle $\Delta\theta_i$ = 4.4 m rad. The number of tracks ΔN_i in each segment is counted. The mean energy E_i in keV and energy increment ΔE_i in keV of each segment are calculated to find the energy spectrum as

$$\frac{dN}{dE} = \frac{\Delta N_i}{\Delta\theta_i}\frac{\Delta\theta_i}{\Delta E_i}$$

and plotted in Fig. 5. The spectrum can be fitted by a power law with two different exponents, $\propto E^{-2}$ and $\propto E^{-3.5}$. It is interesting to note that this power law is similar to that of dense plasma focus produced deuteron beam reported by Gerdin et al.[7] This spectrum, of course, is representative of the ion beam on axis that passed through the 10 μm diameter pinhole of the spectrometer.

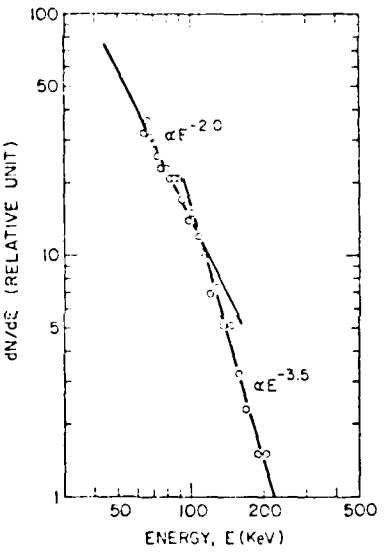

FIG. 5. Proton energy spectrum.

Conclusions

We have shown that high power pulses can be produced by a current charged transmission line and opening switch. A plasma focus, as an opening switch and a diode, has been incorporated with a current charged transmission line to produce energetic charged particles. By analyzing Thomson parabola data, protons and impurity ions have been identified. In addition, the time integrated energy spectrum of the proton beam has been constructed. Although a great deal more effort is required to understand the detailed dynamics of the plasma focus opening switch, it has been demonstrated that the current charged transmission line and plasma focus system is an attractive compact accelerator.

Acknowledgements

The authors would like to thank Professors H. H. Fleischmann and W. W. Destler for their helpful discussions.

References

1. J. H. Nation, Part. Accel. 10, 1 (1979).
2. M. J. Rhee, Bull. Am. Phys. Soc. 27, 1063 (1982).
3. J. P. VanDevender and T. H. Martin, IEEE Trans. Nucl. Sci. 22, 979 (1979).
4. J. W. Mather, Dense Plasma Focus, in Methods of Experimental Physics, 9, Part B, Academic, New York 210, (1971).
5. M. J. Rhee, IEEE Trans. Nucl. Sci. 28, 2663 (1981).
6. M. J. Rhee, NBS Spec. Pub. 628, p. 257 (1982).
7. G. Gerdin, W. Stygar, and F. Venneri, J. Appl. Phys. 52, 3269 (1981).

Presented at International Workshop on Plasma Focus Research
Stuttgart, Germany, September 12-13, 1983

CHARGE STATE RESOLVED ENERGY SPECTRA OF He, N, Ar, AND Ne IONS*

M. J. Rhee, C. M. Luo,+ and R. F. Schneider
Laboratory for Plasma and Fusion Energy Studies
University of Maryland
College Park, MD 20742 U.S.A.

J. R. Smith
Naval Surface Weapons Center
Silver Spring, MD 20910 U.S.A.

Ions of He, N, Ar, and Ne are produced in a plasma focus device with a current charged transmission line, and their charge states are analyzed using a Thomson spectrometer. The charge state resolved energy spectra are constructed for the same ions from the track density distribution on the Thomson parabolas.

Up to a few MeV of ions and electrons, which is many times the product of their charge and the capacitor charging voltage, are observed and reported by many laboratories.[1-5] Similar results are obtained in a pulse powered plasma focus device[6] and a current charged transmission line with a plasma focus opening switch.[7] However, current understanding of the physics in the plasma focus is rather marginal in contrast to the simplicity of the device and clear experimental facts. For this, further experimental studies such as the measurement of energy spectra is suggested. Energy spectra of proton beams,[1,2] deuteron beams,[1-5] and electron beams[5] and some of impurity ions[4] have been reported. The Thomson spectrometer, particularly with a nuclear track detector, is well suited for analysis of ion beams produced in plasma focus.[8,9] In the experimental study reported here, ion beams composed predominantly of fill gas elements of He, N, Ar, and Ne are produced by a plasma focus device with a current charged line. The charge to mass ratio and energy spectra of these ions are analyzed using a compact Thomson spectrometer with CR-39 track detector.

The device used in this experiment to produce the ion beams is very similar to the conventional plasma focus device, except that a transmission line is deliberately inserted between the capacitor and the coaxial plasma gun, as shown in Fig. 1. A 3 kJ, 20 kV capacitor is connected to

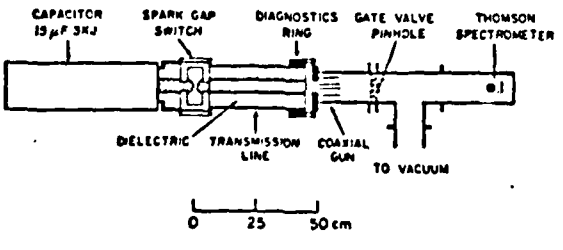

FIG. 1. Experimental configuration.

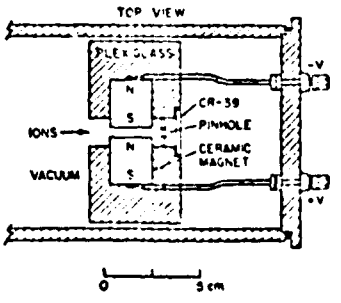

FIG. 2. Compact Thomson spectrometer with CR-39 track detector.

a Mather geometry coaxial electrode of diameters 2a = 2.54 cm, 2b = 7.7 cm, and length ℓ = 10 cm through a transmission line of radii a = 2.54 cm, b = 7.3 cm, and length ℓ = 30 cm, whose total inductance is 64 nH. The characteristic impedance of the transmission line can be varied from 7 to 60 Ω by using different dielectrics in the coaxial transmission line. Water, among the easily available dielectrics, gives the lowest impedance (7 Ω) in the device and has been used throughout this work.

A compact Thomson spectrometer is placed at the end of the downstream drift chamber, which is separated by a special homemade gate-valve of 1.5 mm diameter aperture to maintain a good vacuum for the spectrometer. The spectrometer,[7] the main diagnostic in this study, uses two small permanent bar magnets to produce the magnetic field and also the electric field by biasing them to a high voltage as shown in Fig. 2. Such small magnets for both fields built into the system and the use of CR-39 plastic detector allow us to build a system so compact that the whole system can be fit into any small vacuum chamber. A simple advancing mechanism of the CR-39 detector plate (not shown in the figure) is employed in the system to make multiple exposures on a detector plate without breaking the vacuum.

The system is operated at a typical charging voltage of 18 kV with various fill gases. The spark gap switch is triggered immediately after the gate valve is opened such that the ions accelerated in the focus can pass through the valve to be recorded in the specrometer while the pressure in the gun chamber remains almost unchanged during this short period of time, and a good vacuum is maintained in the downstream spectrometer chamber. The main current through the coaxial line and voltage induced at the time of current disruption are monitored by a Rogowski coil and a D probe respectively, which are mounted on a diagnostic ring placed at the end of the transmission line. Each Thomson spectrogram is constructed by two shots of exposure: one shot with both electric and magnetic fields to produce parabolas and the other shot with

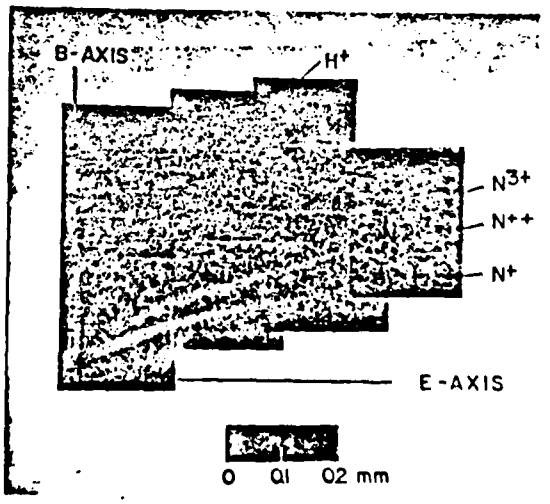

FIG. 3. A typical Thomson spectrogram for Nitrogen.

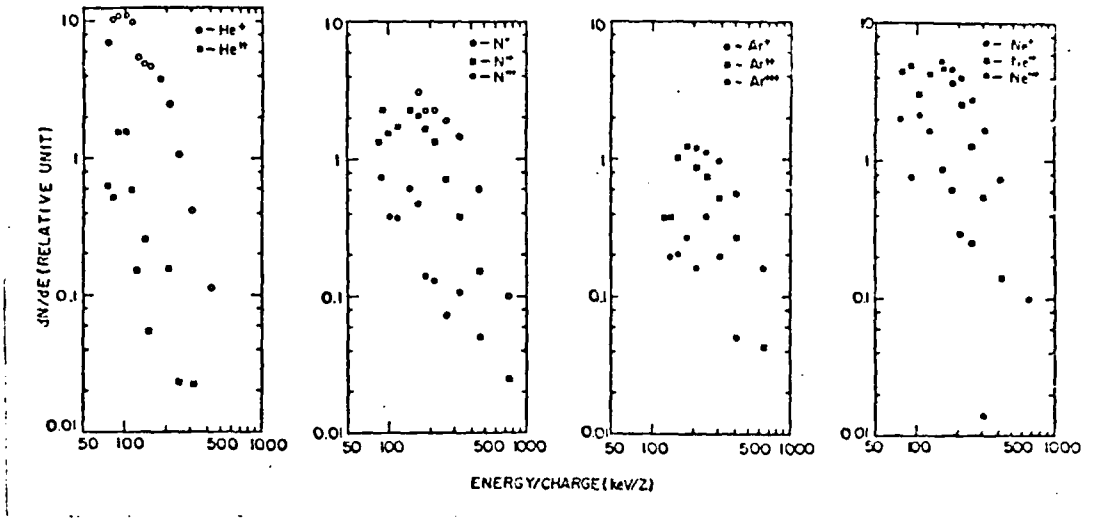

FIG. 4. Charge state resolved energy spectra for He, N, Ar, and Ne ions.

parabolas on CR-39 track detector, the charge state resolved energy spectra are constructed for the same ions. The resulting spectra of different ion species and charge states are similar to each other.

*Work supported by AFOSR, DOE, and IR at NSWC.

+Permanent address: Tsinghua University, Peking, China.

References

1. R. L. Gullickson, W. L. Pickles, D. F. Price, H. L. Sahlin, and T. E. Wainwright, Lawrence Livermore Laboratory, Preprint UCRL-81962 (1979).
2. M. Yokoyama, Y. Kitagawa, Y. Yamada, and C. Yamanaka, Institute of Laser Engineering, Osaka Univ., ILE 8109P (June 1981).
3. G. Gerdin, W. Stygar, and F. Venneri, J. Appl. Phys. 52 (5), 3269 (1981).
4. L. Bertalot, R. Deutsch, H. Herold, U. Jäger, A. Mozer, M. Sadowski, and H. Schmidt, Institut für Plasmaforschung der Universitat Stuttgart, IPF-81-9.
5. W. Stygar, G. Gerdin, F. Venneri, and J. Mandreakas, Nucl. Fusion, 22 (9), 1161 (1982).
6. M. J. Rhee, Appl. Phys. Lett. 37 (10), 906 (1980).
7. M. J. Rhee and R. F. Schneider, IEEE Trans. Nucl. Sci. NS-30, No. 4, 3192 (1983).
8. H. Herold, A. Mozer, M. Sadowski, and H. Schmidt, Rev. Sci. Instrum. 52 (1), 24 (1981).
9. M. J. Rhee, IEEE Trans. Nucl. Sci. NS-28 2663 (1981).
10. R. L. Fleischer, P. B. Price, and R. M. Walker, Nuclear Tracks in Solids (U. of California Press, 1975).
11. M. J. Rhee, to be published.

only the magnetic field to produce a reference axis (B-axis). We have found that neutral particles, identified with the aid of a scanning electron microscope, always exist and conveniently define the origin of the parabola coordinate system from which the E-axis is drawn as shown in Fig. 3. The CR-39 detector is etched in 6.25 N NaOH solution at 70° C after exposure to the ions. The desired etching time varies depending on ion species and observation method. For protons, which make the smallest size of track pit, two hours are needed for comfortable counting of individual tracks by using the optical microscope. The heavier the ions, the less etching time is needed. For the electron microscope, which can improve the counting resolution easily by 10 times and also can identify the ion species by the geometry of the track pit,[10] shorter etching time is desirable and advantageous in general. Spectrograms are obtained for the He, N_2, Ar, and Ne fill gases and are enlarged by using an optical microscope. The Nitrogen parabolas are shown in Fig. 3 as an example.

The charge to mass ratio of unknown ions is found by comparing the magnetic deflection of the ions with that of reference ions at the same electric deflection. In most cases, the protons exist as an impurity and are easily identified. Using the protons as a reference, the charge to mass ratio of the unknown parabola is given by

$$\frac{Z}{A} = \left(\frac{\theta_b}{\theta'_b}\right)^2,$$

where θ_b and θ'_b are the magnetic deflections of the unknown ions and that of protons respectively measured at the same elecric deflection. The parabolas shown in Fig. 3 are analyzed and the resulting charge to mass ratios are very close to that of N^+, N^{++}, and N^{+++} within an error of ~ 1 %.

Since the Thomson parabolas are separated by charge state, one can construct a charge state resolved energy spectra of ions. The electric deflection in the spectrometer is the measure of energy per charge:

$$\frac{mv^2}{2}\frac{1}{Z} = \frac{1}{2}\frac{EL}{\theta_e},$$

where the EL is the ideal electric field over a distance L. This term is replaced with a calibrated constant which is obtained by a few different methods but will be presented elsewhere.[11] The parabolas are divided into many small segments of electric deflection angle $\Delta\theta_i$. The number of tracks ΔN_i in each segment of a parabola of charge state Z is counted. The mean energy E_i and energy increment ΔE_i of each segment is calculated. Then the energy spectrum of ions with charge state Z in the parabola is found as

$$\frac{dN}{dE} = \frac{\Delta N_i}{\Delta\theta_i}\frac{\Delta\theta_i}{\Delta E_i},$$

as a function of energy E_i. The parabolas obtained with other fill gases are also analyzed and their energy spectra are constructed and summarized in Fig. 4.

In conclusion, we have analyzed the charge states of He, N, Ar, and Ne ions by using a Thomson spectrometer. Up to triply ionized ions are found in all species except Helium. By counting the tracks of the

Presented at International Workshop on Plasma Focus Research
Stuttgart, Germany, September 12-13, 1983

STUDY OF ELECTRON BEAM PRODUCTION BY A PLASMA FOCUS*

J. R. Smith
Naval Surface Weapons Center
White Oak, Silver Spring, MD 20910 U.S.A.

C. M. Luo,+ M. J. Rhee, and R. F. Schneider
Laboratory for Plasma and Fusion Energy Studies
University of Maryland
College Park, MD, 20742 U.S.A.

A preliminary investigation of the electron beam produced by a plasma focus device using a current charged transmission line is described. Electron beam currents as high as 10 kA were measured. Interaction of the extracted beam and the filling gas was studied using open shutter photography.

While the majority of plasma focus experiments have addressed the measurement of accelerated ions,[1-6] relatively little attention has been given to extraction of the accelerated electrons and direct measurement of their parameters (e.g., current, energy).[7-9] Such electron measurements are of interest in developing a complete understanding of the high fields present in plasma focus experiments. Also, there may be application of the plasma focus device as a compact particle accelerator for electrons.

The operation of a plasma focus as a compact pulsed accelerator (CPA) for ions has been previously reported.[5] This device uses a plasma focus as an opening switch for a current charged transmission line to produce a fast, high voltage pulse. The CPA consists of: (1) a single energy storage capacitor, (2) a spark gap, (3) a coaxial transmission line, and (4) a Mather geometry coaxial plasma gun. For a capacitor charging volatage of 18 kV, a proton beam with peak energy of 250 keV was observed.

The current charged transmission line has advantages over conventional pulse forming lines in terms of: (1) increased energy storage capability and (2) less stringent constraints on voltage hold-off requirements. Both of these advantages allow the CPA to be more compact than electron accelerators using conventional pulse forming lines.

The CPA, like other plasma focus devices, accelerates ions away from the plasma gun and electrons toward the plasma gun. In the typical plasma focus experiment, the energy storage capacitor bank is connected to the plasma gun with parallel plate transmission lines or cables. Therefore, there are no obstructions which prevent extraction of accelerated electrons out of the rear of the gun if a hollow anode is used. In the CPA geometry, both the capacitor and coaxial transmission line block extraction of electrons. This paper describes CPA operation for electron beam production by use of a new coaxial plasma gun design. The beam was fired into a drift region containing the same gas environment as the plasma gun. In this region, preliminary measurements were performed on the electron beam.

Main components of the CPA are shown in Fig. 1. The energy storage capacitor (15 μF, 3 kJ) was typically charged to 18 kV. Charging of the coaxial transmission line was initiated by a high voltage trigger pulse (30 kV) which was applied to a needle electrode inserted at the midplane of the spark gap. The water filled coaxial transmission line (inner radius 2.54 cm, outer radius 7.3 cm, length 30 cm) has an impedance of 7 Ω. A diagnostics ring connected on the end of the transmission line contains a Rogowski coil and capacitive voltage probe. The Rogowski coil measures the main current (I_m) through the coaxial line, and the capacitive probe measures the voltage induced at the time of current disruption. Theory of operation for the CPA is found in Ref. 5.

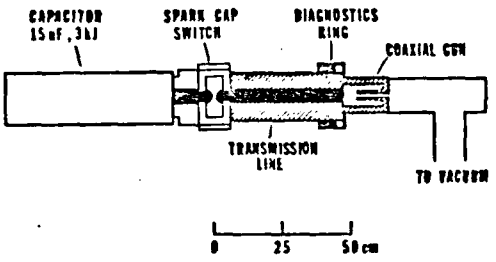

FIG. 1. The compact pulsed accelerator.

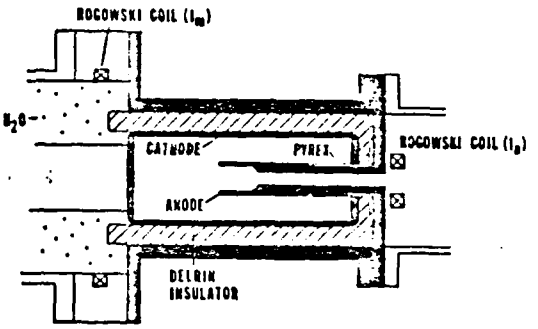

FIG. 2. Plasma focus gun.

A new plasma gun design which allows extraction of electrons from the CPA is shown in Fig. 2. The copper electrodes have the same dimensions as those used for the ion experiments (i.e., 2.54 cm diameter anode, 7.7 cm diameter cathode) and are separated by a pyrex insulator. The center conductor of the transmission line (charged negatively) is attached to the outer conductor (cathode) of the plasma gun. The outer conductor of the transmission line is folded inward to become the center conductor (anode) of the plasma gun. The plasma gun section was designed so its characteristic impedance would match the 7 Ω impedance of the water filled transmission line. Electrons are extracted out of the hollow anode through a 9 mm diameter aperture and enter a 10 cm diameter drift region filled with the same gas as the plasma gun. Filling gases of H_2, He, N_2, or Ar were used. Typical current and voltage waveforms measured with the diagnostics ring are shown in Fig. 3.

A second Rogowski coil placed at the drift tube entrance measured the apparent current (I_a). Although this diagnostic gives a good approximate representation of the actual electron beam current pulse (Fig. 4), plasma return currents may alter the pulse's height and length. The peak apparent current vs. gas pressure for He, N_2, and Ar is shown in Fig. 5. While peak currents were generally several kiloamperes, in a few shots currents of 10 kA were observed. Actual beam currents may be much greater since the beam is extracted through such a small aperture (9 mm). The most reproducible current pulses were obtained with argon gas, where the leading edge of the electron beam pulse always coincided with the interruption of the main focus current. This was not true with the lighter gases, where in some cases even multiple pulses were

detected. Higher peak currents were observed in the lower pressure range for all gases.

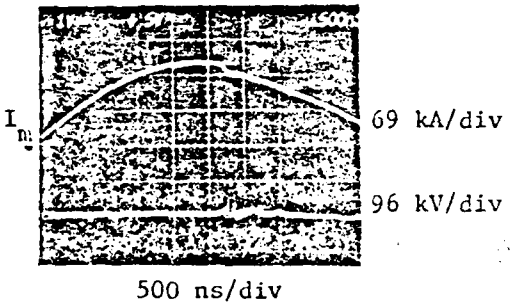

FIG. 3. Current and voltage waveforms for the compact pulsed accelerator.

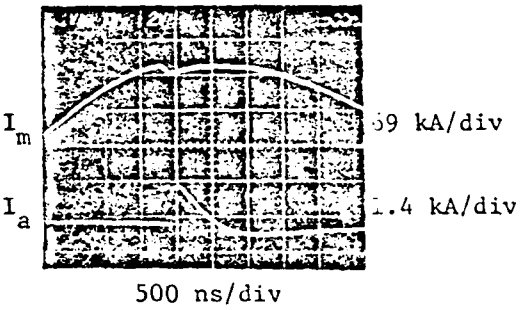

FIG. 4. Oscilloscope trace of the apparent current measured by the Rogowski coil placed in the drift tube.

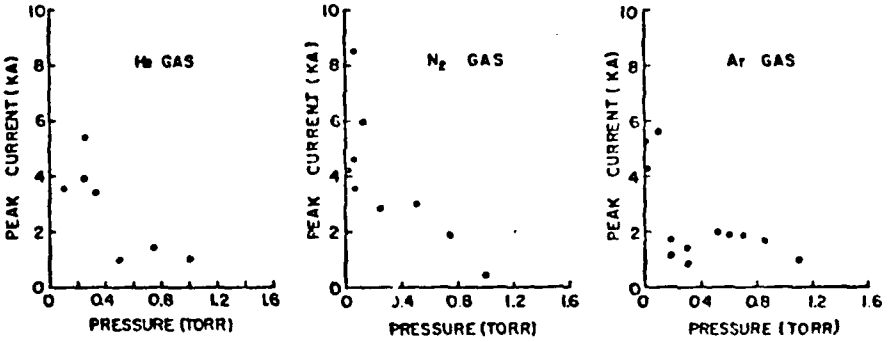

FIG. 5. Plots of peak measured current (I_a) vs. gas pressure for He, N_2, and Ar.

Open shutter photographs were made for observation of the interaction between the electron beam and filling gas. An acrylic tube with a copper mesh insert was attached between the plasma gun and vacuum pumping section for this series of shots. Observation of the beam-gas interaction over a broad pressure range (0 ~ 2 torr Ar) revealed two distinct propagation regimes as shown in Fig. 6. The structure observed in the low pressure shot of Fig. 6 was very reproducible throughout the low pressure regime. These measurements will aid in placement of beam-diagnostics and interpretation of their results in future work.

The compact pulsed accelerator has been successfully operated in the electron beam mode. The beam produced by the focus has a peak current density of 15 kA/cm^2 which is comparable to intense beams produced by much larger electron accelerators. A heavy gas (Ar) was found more efficient for providing a reproducible electron beam. Light gases supply light ions which can be more easily accelerated across the plasma opening switch, thereby decreasing the efficiency of electron acceleration. For the current pulses which were coincident with interruption of the focus

current, the acceleration can be linked to the fields created by the plasma focus opening switch. Future work will include measurement of the electron energy spectrum and a comparison with expected magnitude of the plasma focus fields.

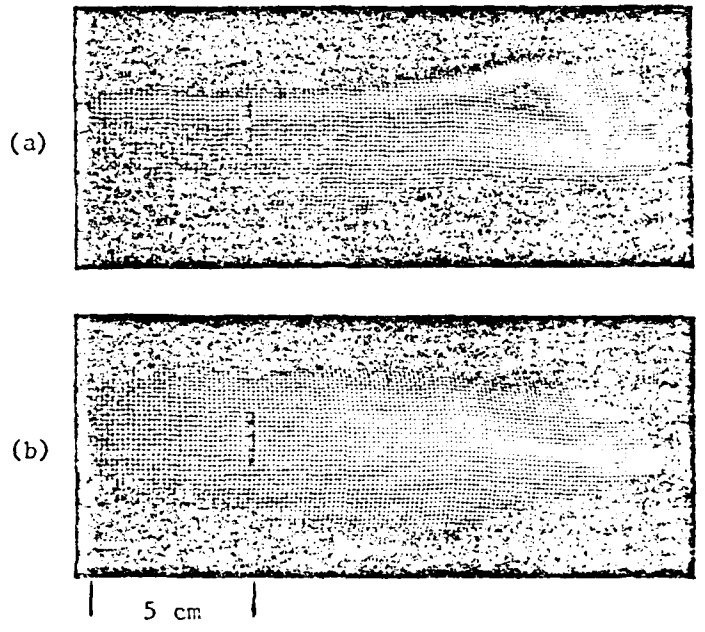

Fig. 6. Open shutter photographs of electron beam injection into a gas filled drift tube. Results of (a) 0.4 torr Argon and (b) 1.6 torr Argon are shown.

*Work supported by AFOSR, DOE, and IR at NSWC.
+Permanent address: Tsinghua University, Peking, China.

References

1. R. L. Gullickson and H. L. Sahlin, J. Appl. Phys. 49, 1099 (1978).
2. M. J. Rhee, Appl. Phys. Lett. 37, 906 (1980).
3. A. Mozer, M. Sadowski, H. Herold, and H. Schmidt, J. Appl. Phys. 53, 2959 (1982).
4. G. Gerdin, W. Stygar, and F. Venneri, J. Appl. Phys. 52, 3269 (1981).
5. M. J. Rhee and R. F. Schneider, IEEE Trans. Nucl. Sci. 30, 3192 (1983).
6. Y. Kitagawa, Y. Yamada, A. Ishizaki, M. Naito, M. Yokoyama, and C. Yamanaka, 1980 IEEE Int. Conf. on Plasma Sci. Conf. Record-Abstracts, IEEE Catalog No. 80CH1544-6 NPS (1980) 74.
7. W. H. Bostick, V. Nardi, W. Prior, J. Feugeas, H. Kilic, and C. Powell, Bull. Am. Phys. Soc. 23, 848 (1978).
8. G. M. Molen, ibid, 74.
9. W. Stygar, G. Gerdin, F. Venneri, and J. Mandrekas, Nucl. Fusion 22, 1161 (1982).

APPENDIX B

List of Publications and Reports Resulting from this Contract

APPENDIX B

LIST OF PUBLICATIONS AND REPORTS RESULTING FROM THIS CONTRACT

1. W. W. Destler, L. E. Floyd, and M. Reiser, "Collective Acceleration of Heavy Ions," Phys. Rev. Lett. 44, 70 (1980).

2. W. W. Destler, "Collective Ion Acceleration from a Localized Ion Source, invited paper, 2nd Int. Conf. on Energy Storage, Compression & Switching, December 5-8, 1978, Venice, Italy.

3. W. W. Destler, L. E. Floyd, and M. Reiser, "Experimental Studies of Heavy Ion Collective Acceleration at the University of Maryland," IEEE Trans. Nucl. Sci. 26, (1979).

4. A. Sternlieb, H. S. Uhm, W. W. Destler, and M. Reiser, "A Time Dependent Study of Linear Collective Ion Acceleration," Bull. Am. Phys. Soc. 24 (9), (1979).

5. L. E. Floyd, W. W. Destler, M. Reiser, A. Sternlieb, H. M. Shin, and S. W. Graybill, "Collective Acceleration of Heavy Ions," Bull. Am. Phys. Soc. 24 (9), (1979).

6. L. E. Floyd, W. W. Destler, M. Reiser, and H. M. Shin, "Experimental Study of Collective Acceleration of Ions from a Localized Gas Cloud," J. Appl. Phys. 52, 693 (1981).

7. J. T. Cremer, W. W. Destler, L. E. Floyd, M. Reiser, and C. J. Shedlock, "Collective Acceleration of Laser-Produced Ions," Bull. Am. Phys. Soc. 25 (8), (1980).

8. L. E. Floyd, W. W. Destler, M. Reiser, and H. M. Shin, "Experimental Studies of Collective Acceleration of Ions From a Localized Gas Cloud," Bull. Am. Phys. Soc. 25 (8), (1980).

9. R. R. Kulkarni, "Theoretical Studies of Helix Controlled Beam Front Collective Ion Acceleration," M.S. Thesis, University of Maryland, 1980.

10. J. M. Grossmann, R. Kulkarni, C. D. Striffler, and R. Faehl, "Virtual Cathode Dynamics in 2D Geometry--1D Momentum Space," Proc. Ninth Conf. on Numerical Simulation of Plasmas, Northwestern University, Evanston, IL, 1980.

11. M. J. Rhee, "Thomson Spectrometer Measurement of Heavy Ion Beams Produced by a Pulse Powered Plasma Focus Device," Proc. Workshop on Measurement of Electrical Quantities in Pulsed Power Systems, Boulder, CO, 1981.

12. W. W. Destler, L. E. Floyd, J. T. Cremer, C. R. Parsons, M. Reiser, and J. W. Rudmin, "Collective Acceleration of Light and Heavy Ions," IEEE Trans. Nucl. Sci. 28, 3404 (1981).

13. M. J. Rhee, "Fully Stripped Ion Beams Produced by Pulse Powered Plasma Focus Device," IEEE Trans. Nucl. Sci. 28, 2663 (1981).

14. J. M. Grossmann, I. Mayergoyz, and C. D. Striffler, "Theoretical Studies of Collective Ion Acceleration in a Linear Beam-Evacuated Drift Tube System," IEEE Trans. Nucl. Sci. 28, 2587 (1981).

15. M. Reiser, "Recent Advances in Collective Ion Accelerators," invited paper, 1981 Particle Accelerator Conference, IEEE Trans. Nucl. Sci. 28, 3355 (1981).

16. C. D. Striffler, I. Mayergoyz, and J. M. Grossmann, "Theoretical Considerations of the Collective Ion Accelertion Studies at the University of Maryland," Proc. of 4th Int. Topical Conf. on High-Power Electron and Ion-Beam Res. and Tech., Palaiseau, France, 1981.

17. W. W. Destler, L. E. Floyd, J. T. Cremer, C. R. Parsons, and M. Reiser, "Collective Ion Acceleration Studies at the University of Maryland," Proc. 4th Int. Topical Conf. on High-Power Electron and Ion-Beam Res. and Tech. Palaiseau, France, 1981.

18. M. J. Rhee, "Acceleration of Charged Particle in Plasma Focus," IEEE Conf. Record-Abstracts, 1981, IEEE Int. Conf. on Plasma Sci. p. 121, Santa Fe, NM, 1981.

19. M. J. Rhee, "Peak Energie: of Charged Particles Accelerated in Plasma Focus," Bull. Am. Phys. Soc. 26 (7), 893 (1981).

20. J. M. Grossmann, H. Dantsker, I. Mayergoyz, and C. D. Striffler, "A Collective Ion Acceleration Model for Linear Beam-Evacuated Drift Tube Systems," Bull. Am. Phys. Soc. 26, 1036 (1981).

21. W. W. Destler, I. D. Mayergoyz, and F. P. Emad, "Application of Intense Relativistic Electron Beams to the Switching of High Currents in High Power Electrical Networks," J. Appl. Phys. 53, 7189 (1982).

22. W. W. Destler, "Production of Positron Emitting Isotopes Using a Collective Accelerator," Rev. Sci. Inst. 54, 253 (1982).

23. M. Reiser, "High Energy Accelerators and Collective Accelerators," invited paper, Capri Summer Seminar on "Future Trends of Accelerators," June 1-3, 1982.

24. W. W. Destler and M. Reiser, "Alternatives to Cyclotrons for the Production of Radioisotopes for Positron Emission Tomography: Collective Accelerators," 1982 IEEE Int. Conf. on Plasma Science, Ottawa, Ontario, Canada, May 17-19, 1982.

25. J. T. Cremer, H. Dantsker, W. W. Destler, L. E. Floyd, J. M. Grossmann, R. Kulkarni, I. Mayergoyz, M. Reiser, and C. D. Striffler, "Collective Acceleration of Light and Heavy Ions," 1982 IEEE Int. Conf. on Plasma Science, Ottawa, Ontario, Canada, May 17-19, 1982.

26. C. R. Parsons and M. J. Rhee, "Energy Analysis and Track-Plate Detection of Laser-Produced Ions," 1982 IEEE Int. Conf. on Plasma Science, Ottawa, Ontario, Canada, May 17-19, 1982.

27. M. J. Rhee and A. Shpilman, "Thomson Spectrometer and Nuclear Track Analysis of Ions Produced by Pulse Powered Plasma Focus Device," 1982 IEEE Int. Conf. on Plasma Science, Ottawa, Ontario, Canada, May 17-19, 1982.

28. J. M. Grossmann, "Numerical Study of Virtual Cathode Behavior in Vacuum Collective Ion Acceleration Systems," Ph.D. Thesis, University of Maryland, 1982.

29. J. M. Grossmann, R. Kulkarni, I. Mayergoyz, and C. D. Striffler, "Theoretical Study of Virtual Cathode Behavior in Vacuum Collective Ion Acceleration Systems," to be submitted to J. Appl. Phys., Oct. 1983.

30. W. W. Destler and J. T. Cremer, "Charge State Measurements of Collectively Accelerated Heavy Ions," J. Appl. Phys. 54, 636 (1982).

31. P. G. O'Shea, W. W. Destler, C. D. Striffler, and D. Welsh, "Helix Controlled Collective Ion Acceleration," Bull. Am. Phys. Soc. 27 (8), (1982).

32. J. T. Cremer and W. W. Destler, "A Study of Laser Produced Plasma from Solid and Foil Metal Targets," Bull. Am. Phys. Soc. 27 (8), (1982).

33. C. D. Striffler, H. Dantsker, "Collective Ion Acceleration in Linear Beam-Localized Gas Cloud Systems," Bull. Am. Phys. Soc. 27, (1982).

34. M. J. Rhee, "A Simple High Power Pulse Forming System: Current Charged Transmission Line with Plasma Focus Opening Switch," Bull. Am. Phys. Soc. 27, 1063 (1982).

35. A. Shpilman and M. J. Rhee, "Identification of Ion Species Produced by a Pulse Powered Plasma Focus Switch," Bull. Am. Phys. Soc. 27, 1063 (1982).

36. M. J. Rhee and R. F. Schneider, "Compact Pulsed Accelerator," IEEE Trans. Nucl. Sci. 30, 3192 (1983).

37. M. J. Rhee and R. F. Schneider, "Measurements of Ions Produced by a Current Charged Transmission Line with Plasma Focus Opening Switch," IEEE Conference Record-Abstracts, 1983 IEEE Int. Conf. on Plasma Science, p. 59, San Diego, CA (May 1983).

38. M. J. Rhee, C. M. Luo, R. F. Schneider, and J. R. Smith, "Charge State Resolved Energy Spectra of He, N, Ar, and Ne Ions," Presented at Int. Workshop on Plasma Focus Research, Stuttgart, Germany (Sept. 1983), to be published in Proceedings of the Workshop.

39. J. R. Smith, C. M. Luo, M. J. Rhee, and R. F. Schneider, "Study of Electron Beam Production by a Plasma Focus," Presented at Int. Workshop on Plasma Focus Research, Stuttgart, Germany (Sept. 1983), to be published in Proceedings of the Workshop.

40. M. J. Rhee, C. M. Luo, R. F. Schneider, and J. R. Smith, "Thomson Spectrometer Analysis and Energy Spectra for Heavy Ions Produced by Current Charged Line with Plasma Focus," Bull. Am. Phys. Soc. 28, 1171 (1983).

41. R. F. Schneider, C. M. Luo, M. J. Rhee, and J. R. Smith, "Ion Beam Production Efficiency in a Plasma Focus," Bull. Am. Phys. Soc. 28, 1172 (1983).

42. C. M. Luo, M. J. Rhee, R. F. Schneider, and E. S. Sim, "Compact Thomson Parabola Analyzer and Magnetic Electron Analyzer," Bull. Am. Phys. Soc. 28, 1070 (1983).

43. L. E. Floyd, "Experimental Study of Collective Acceleration of Light and Heavy Ions from a Localized Gas Cloud," Ph.D. Thesis, October 1983.

44. W. W. Destler, P. G. O'Shea, M. Reiser, C. D. Striffler, and H. H. Fleischmann, "Studies of the Helix Controlled Beam Front Accelerator Concept," IEEE Trans. Nucl. Sci. 30, 3183 (1983).

45. J. T. Cremer and W. W. Destler, "Collective Acceleration of Laser Produced Ions," IEEE Trans. Nucl. Sci. 30, 3186 (1983).

46. M. Reiser and W. W. Destler, "Generation of Charge-Neutral, Current-Neutral, Charged Particle Beams," Bull. Am. Phys. Soc. 28, 1038 (1983).

47. D. Welsh, C. D. Striffler, P. G. O'Shea, and W. W. Destler, "Limiting Currents of a Solid Relativistic Electron Beam," Bull. Am. Phys. Soc. 28, 1039 (1983).

48. J. T. Cremer, W. W. Destler, L. E. Floyd, P. G. O'Shea, and M. Reiser, "Experimental Studies of Collective Ion Acceleration at the University of Maryland," Bull. Am. Phys. Soc. 28, 1141 (1983).

49. W. W. Destler, P. G. O'Shea, and M. Reiser, "Electron Beam Propagation through a Localized Plasma into Vacuum," (submitted to Phys. Rev. Lett., October 1983).

50. W. W. Destler, P. G. O'Shea, and M. Reiser, "Propagation of an Intense Relativistic Beam through a Plasma Region into Vacuum," (submitted to Phys. Fluids, October 1983).

51. P. G. O'Shea, D. Welsh, W. W. Destler, and C. D. Striffler, "Intense Relativistic Electron Beam Propagation in Evacuated Drift Tubes," (submitted to J. Appl. Phys., October 1983).

52. M. Reiser, "Beam Front Accelerators," ECFA-RAL Meeting, "The Challenge of Ultra-High Energies," Oxford, England, Sept. 27-30, 1982.


DAT
ILM